Histol Histopathol (2024) 39: 177-200

Histology and Histopathology
From Cell Biology to Tissue Engineering

ORIGINAL ARTICLE Open Access

Spatial transcriptomic analysis of tumour with high and low CAIX expression in TNBC tissue samples using GeoMx™ RNA assay

Suad A.K. Shamis[1,2], Francesca Savioli[1], Aula Ammar[2], Sara S.F. Al-Badran[2], Phimmada Hatthakarnkul[2], Holly Leslie[2], Elizabeth E.A. Mallon[3], Nigel B. Jamieson[2], Donald C. McMillan[1] and Joanne Edwards[2]

[1]Academic Unit of Surgery, School of Medicine, University of Glasgow, Royal Infirmary, Alexandria Parade, [2]Unit of Molecular Pathology, School of Cancer Sciences, University of Glasgow, Wolfson Wohl Cancer Research Centre, Garscube Estate and [3]Department of Pathology, Queen Elizabeth University Hospital, Glasgow, United Kingdom

Summary. Purpose. Prognostic significance and gene signatures associated with carbonic anhydrase IX (CAIX) was investigated in triple negative breast cancer (TNBC) patients.

Methods. Immunohistochemistry (IHC) for CAIX was performed in tissue microarrays (TMAs) of 136 TNBC patients. In a subset of 52 patients Digital Spatial Profiler (DSP) was performed in tumour (pan-cytokeratin+) and stroma (pan-cytokeratin-). Differentially expressed genes (DEGs) with $P<0.05$ and log2 fold change (FC)>(±0.25 and ±0.3, for tumour and stromal compartment, respectively) were identified. Four genes were validated at the protein level.

Result. Cytoplasmic CAIX expression was independently associated with poor recurrence free survival in TNBC patients [hazard ratio (HR)=6.59, 95% confidence interval (CI): 1.47-29.58, P=0.014]. DEG analysis identified 4 up-regulated genes (CD68, HIF1A, pan-melanocyte, and VSIR) in the tumour region and 9 down-regulated genes in the stromal region (CD86, CD3E, MS4A1, BCL2, CCL5, NKG7, PTPRC, CD27, and FAS) when low versus high CAIX expression was explored. Employing IHC, high CD68 and HIF-1α was associated with poorer prognosis and high BCL2 and CD3 was associated with good prognosis.

Conclusions. DSP technology identified DEGs in TNBC. Selected genes validated by IHC showed involvement of CD3 and BCL2 expression within stroma and HIF-1α, and CD68 expression within tumour. However, further functional analysis is warranted.

Corresponding Author: Suad A.K. Shamis, Academic Unit of Surgery, School of Medicine, University of Glasgow, Royal Infirmary, Alexandria Parade, G31 2ER, Glasgow, UK. e-mail: S.Shamis.1@research.gla.ac.uk

www.hh.um.es. DOI: 10.14670/HH-18-655

Key words: Breast cancer, CAIX, Hypoxia gene expression, Nanostring nCounter techonology transcriptomics, HIF-1α, Apoptosis; BCL2, Infiltrating macrophages; CD68, Lymphocytes; CD3, Stromal microenvironment

Introduction

Breast cancer (BC) is a common and life-threatening disease in women (Bray et al., 2018), and it is the second leading cause of death in women (Lei et al., 2021). It is a highly heterogeneous disease, however clinic-pathological factors as well as multi-genomic assays can be utilised to classify BC into three clinical subtypes: hormone-receptor-positive, human epidermal growth factor receptor 2, and triple negative breast cancer (TNBC) (Goldhirsch et al., 2013). TNBC is characterised by the absence of oestrogen receptor (ER), progesterone receptor (PR) and human epidermal growth factor receptor 2 (Her-2) and accounts for about 15-20% of all BCs. It is associated with a higher mortality rate than the other subtypes of BC (Nwagu et al., 2021). Currently, no TNBC targeted therapy has been approved

Abbreviations. CAIX, Carbonic anhydrase IX; TNBC, Triple negative breast cancer; IHC, Immunohistochemistry; FFPE, Formalin-fixed paraffin-embedded tissue; TMAs, Tissue microarrays; DSP, Digital Spatial Profiler; PanCK, Pan-cytokeratin; DEGs, Differentially expressed genes; BC, Breast cancer; ER, Oestrogen receptor; PR, Progesterone receptor; TME, Tumour microenvironment; HR, Hazard ratio; 95%CI, 95% confidence interval; HIF-1α, Hypoxia-inducible factor-1α; BCL2, B-cell lymphoma-2; ICCC, Interclass correlation coefficient; RFS, Recurrence free survival; DFS, Disease free survival; OS, Overall survival; AOI, Area of illumination; ROI, Region of interest; QC, Quality control; TIL, Tumour infiltrating lymphocyte; TAM, Tumour associated macrophage; IL-2, Interleukin-2; IFNγ, Interferon-γ; TNF, Tumour necrosis factor

despite the large number of studies and clinical trials (Bianchini et al., 2016). However, genes dysregulated in TNBC could be a potential therapeutic target.

The role of the tumour microenvironment (TME) in cancer progression is thought to be crucial. It has been implicated in immune suppression and evasion (Hanahan and Weinberg, 2011). Tumour associated macrophages (TAMs) play an important immunosuppressive role by secreting inhibitory cytokines, promoting regulatory T cell infiltration, and reducing reactive oxygen species (Ahn et al., 2017). TNBCs feature a unique microenvironment, distinct from that of other BC subtypes (Yu and Di, 2017). In fact, there is remarkable heterogeneity of the TME among different RNA-based TNBC subtypes (Bareche et al., 2020). The TME associated with response to treatment and prognosis of TNBC (Loi et al., 2014; Denkert et al., 2018). Therefore, an increasing number of studies have focused on the TME to identify new biomarkers or target stromal components to predict clinical outcome and guide therapy in TNBCs (Matsumoto et al., 2015). Bioinformatics methods can be used to interrogate the mutational and gene expression profiles that underlie TNBC and elucidate the molecular mechanism that drive pathogenesis (Li et al., 2018).

Hypoxia is identified as a hallmark of the TME (Kim et al., 2018) and a common characteristic of most solid tumours (Shao et al., 2018). Hypoxia is involved in biological processes promoting tumour progression and stabilises hypoxia-inducible factor-1α (HIF-1α), thereby stimulating expression of a large battery of genes (Semenza, 2003). Carbonic anhydrase IX (CAIX), a transmembrane glycoprotein, is a HIF-1α -responsive metalloenzyme (Beasley et al., 2001). It stabilizes intracellular pH via catalysing a hydration of extracellular CO_2 molecules to HCO_3^- and H^+ ions. CAIX is highly expressed in a wide spectrum of human cancers, including BC, but not in normal tissue (Thiry et al., 2006), and it is associated with poor prognosis in TNBC (Jin et al., 2016; Cui and Jiang, 2019). CAIX protein as a biomarker for hypoxia could be more suitable as it is more stable and persists longer than HIF-1α (Lal et al., 2001). This further supports that HIF-1α may not be an exclusive candidate marker for BC.

Although there is an increasing awareness that tumour and stromal interactions contribute to tumour progression, previous studies have not addressed how changes occurring in tumour hypoxia affect disease outcome. In this study, therefore, GeoMx digital spatial profiler (DSP) was used to explore potential biomarkers of hypoxic TNBC. We examined the applicability of GeoMx DSP technique to the analysis of cytoplasmic CAIX protein expression in TNBC samples. Such insight is essential to identify new therapeutics targeting hypoxic tumour cells and the hypoxic micro-environment.

Materials and methods

The present study was performed in three steps: (1) Immunohistochemistry (IHC) of CAIX in TNBC cohort, (2) Spatial analysis of RNA transcripts in tumour tissues, (3) Validation of genes at protein level by IHC.

Patient cohort

Cores of 0.6 mm from formalin-fixed paraffin-embedded (FFPE) tissue microarrays (TMAs) blocks were obtained from 207 TNBC patients, who underwent surgery in the West of Scotland at the Greater Glasgow and Clyde, between 2011 and 2019. 136 patients remained for downstream IHC analysis after excluding patients who did not have ductal carcinoma or CAIX expression was unavailable (n=30), and who received neoadjuvant chemotherapy (n=41) as showed in Figure 1A.

TMA cores from 52 patients, two cores per patient (155 AOI) were utilised for GeoMx DSP analysis. The use of the epithelial cell-specific marker, pan-cytokeratin, assists pathologic identification of breast tumour tissue within a sample. Within these specifications, there were 73 pan-cytokeratin positive (PanCK+) and 82 pan-cytokeratin negative (PanCK-) (Fig. 1B).

All tumour samples were collected following the approval by The Research Ethics Committee of West Glasgow University Hospitals (NHS GG&C REC reference: 16/WS/0207).

Tissue microarrays and immunohistochemistry

To validate the prognostic value of CAIX in TNBC, and to validate DSP genes, HIF-1α, BCL2, CD68, CD3 expression, IHC was carried out using 2.5 μm thick sections of FFPE TNBC tissues.

For CAIX and HIF-1α immunostaining, slides were deparaffinized, rehydrated, and subsequently subjected to heat induced antigen retrieval by immersing them,

Table 1. Antibodies and staining techniques used in the study.

Target	Clone	Origin	Manufacturer	Dilution	Antigen retrieval buffer	Expected staining	Blocking conditions
CAIX	Monoclonal	Mouse	Bioscience	1:500	Citrate pH 6	Cytoplasmic and membrane	10% casein 60 min
HIF-1α	Monoclonal	Mouse	Novus Biologicals	1:150	Tris-EDTA pH 9	Cytoplasmic and nuclear	1.5% horse serum 60 min
BCL2	Monoclonal	Mouse	Agilent	1:150	Tris-EDTA pH 9	Cytoplasmic	-
CD68	Monoclonal	Mouse	DAKO	1:200	HIER Buffer pH 9	Cytoplasmic	200 μl of UVQ (Ultravision Quanto) protein 5 min
CD3	Monoclonal	Mouse	Leica	1:100	HIER Buffer pH 9	Cytoplasmic	200 μl of UVQ protein 5 min

depending on the antibody, either in a water bath with citrate buffer (pH 6), or an EDTA buffer (pH 9). The slides were then incubated with primary antibodies specific for HIF-1α and CAIX after blocking endogenous peroxidase by using 3% hydrogen peroxide (H_2O_2) and non-specific binding by using protein block. Details of the used antigen retrieval buffer, blocking solution, and primary antibodies are listed in Table 1. Antibodies were detected with 3-3'-diaminobenzidine substrate (DAB) as the chromogen (Vector Laboratories), and counterstained with Haematoxylin Gill III (Leica Microsystems, Milton Keynes, UK cat. No. 3801540E).

For BCL2 staining, FFPE sections were loaded into an Agilent pre-treatment module to be dewaxed and heated to 97°C for 20 minutes in target retrieval solution (TRS) (K8004, Agilent) using EDTA buffer (pH 9). Sections then rinsed in flex wash buffer (K8007, Agilent) prior to being loaded onto a Dako Autostainer. The sections underwent peroxidase blocking (S2023, Agilent) before incubated with BCL2 antibody. Antibody details are shown in Table 1. Liquid DAB (K3468, Agilent) was applied to the slides, then sections were washed in water and counterstained with haematoxylin z (RBA-4201-00A, CellPath).

For CD68 and CD3 immunostaining, slides were incubated at 97°C for 30 minutes with the dewax and antigen retrieval buffer H (Epredia) pH 9 using PT module. CD68 and CD3 staining was performed using the Ultravision Quanto kit (Epredia) according to manufacturer instructions. In brief, endogenous peroxidase was blocked by 3% H_2O_2 and non-specific binding blocked by protein block treatment for 5 minutes. After incubation with primary antibodies for 30 minutes, an amplifier treatment for 10 minutes, and HRP treatment for 10 minutes was performed. Details of antibodies, and dilution factors can be found in Table 1. Finally, slides were stained with DAB and counterstained with haematoxylin using the Myreva Autostainer.

Before all slides were mounted, all sections were dehydrated in alcohol and xylene. All samples had a negative control slide (no primary antibody) to assess the degree of non-specific staining, and these were all negative.

Stained slides were digitally scanned using a Hamamatsu NanoZoomer Digital Slide Scanner (Hamamatsu Photonics K.K., Shizuoka, Japan), at 20× magnification high resolution images and viewed using NDP serve 3 image viewer platform system.

Pathological scoring of immunohistochemistry

Assessment of IHC-stained sections by the presence of brown coloured reaction in the membrane/nucleus and/or cytoplasm was considered a positive reaction. Different scoring methods were required to be most appropriate to the biomarker. Expression of protein levels was assessed at each cellular compartment separately. Scoring was performed by a single observer (S.S.) blinded to patient clinical and survival data. Expression of HIF-1α and CAIX was assessed in tumour cells to evaluate hypoxia, BCL2 expression was used to evaluate apoptosis, CD68 expression identified macrophages, and CD3 expression used to measure lymphocytes in 136 included cases.

QuPath scoring

Cytoplasmic CAIX, cytoplasmic and nuclear HIF-1α, cytoplasmic BCL2, and cytoplasmic CD3 expression were scored using QuPath digital pathology software v0.2.3 (QuPath, Edinburgh, UK). In brief, after using the TMA Dearrayer function to create a TMA grid with cores in their correct positions, stain vectors were estimated during pre-processing by the visual stain editor available in QuPath, to increase staining quality. Then, cells were detected using a watershed cell detection method, and annotations were made to allow QuPath to recognise different tissue types which are tumour and stroma. Then, a random trees classifier was trained using over 40 features such as perimeter, area, and optical density. Three intensity thresholds were used to represent negative, weak, moderate, and strong staining, and after the classifier was built, the auto-update feature was used to re-validate the classifier's accuracy in real-time. The classifier was then saved and applied to all TMA slides that were subjected to QuPath analysis (Bankhead et al., 2017). To ensure reproducibility of scoring, 10% of TMA cores for the four markers was co-scored by a second observer (S.A) blinded to the previous observer score as well as patient clinical and survival data.

Weighted histoscore

QuPath was unable to accurately score the membrane CAIX staining, therefore, it was assessed using the manual weighted histoscore method. The weighted histoscore grades staining intensity as negative (0), weak (1), moderate (2), and strong (3), and then multiplies the percentage of tumour cells within each category (Kirkegaard et al., 2006; Wu et al., 2019). The histoscore range is from 0 (minimum) to 300 (maximum). 10% of TMA cores for membranous CAIX was co-scored by a second observer (S.A.) blinded to the previous observer score to ensure reproducibility of scoring.

Manual quantification

QuPath method was inappropriate to score macrophages due to shape irregularity. Therefore, cytoplasmic CD68+ stained cells were quantified manually. The number of CD68+ cells was counted in each tumour rich core and stroma rich core without any previous knowledge of the patients' clinical data. CD68+ cells were counted for each of the cores, in tumour nests, in the TME and finally the total number of CD68+ cells were determined by adding up the counts for tumour

nest and TME. To ensure reproducibility of scoring, 10% of cores for CD68+ marker was co-scored by a second observer (A.A.) blinded to the previous observer score as well as patient clinical and survival data.

Expression of each marker within the cohort was assessed in the three separate tumour/stroma sites. The mean number of triplicate cores from the same tumour/stroma cores was then used for analysis.

Klintrup-Makinen Grading

Klintrup-Makinen (KM) grading was performed as previously described in colorectal cancer (Klintrup et al., 2005). Briefly, H&E-stained sections were assessed at the deepest point of tumour invasion for the broad inflammatory infiltrate on a scale of 0 to 3. Tumours were graded 0 if there were no immune cells present and 1 if a patchy band of immune cells was seen. Tumours with a prominent thin band of inflammatory cells were graded 2 and those with a thicker florid cup of immune cells were graded 3. Patients graded 0 or 1 were classed as low (0) and patients graded 2 or 3 were graded high (1) for inflammatory infiltrate.

Statistical analyses

Agreement between observers was calculated using interclass correlation coefficient (ICCC). Values above 0.75 are indicative of good reliability (Koo and Li, 2016). The optimal threshold for each marker in each cellular compartment was defined using Survminer package in R Studio (RStudio, Boston, MA, USA) based on overall survival (OS). Chi-square test was used to assess the association and distribution of

Table 2. List of genes in GeoMx immune panel.

Target Group	Target name
Cytokine & Chemokine Signaling	STAT1
Background	NegPrb2
Myeloid;Myeloid Supression	IDO1
Cytokine & Chemokine Signaling	STAT3
Myeloid	CD47
T cell Activation;Myeloid;Checkpoint	CD86
Immune Cell Adhesion & Migration	ITGAV
Cytokine & Chemokine Signaling	CXCR6
Background	NegPrb1
Myeloid Activation;Cytokine & Chemokine Signaling;Myeloid	CSF1R
Antigen Presentation;MHC2	CD74
Proliferation	CCND1
Myeloid Activation;Checkpoint	CD274
Myeloid Activation;Myeloid	CD40
Melanoma	pan-melanocyte
Cytokine & Chemokine Signaling	IL6
T cells;CD8 T cells	CD8A
Background	NegPrb3
B cells	MS4A1
B cells;Myeloid;Checkpoint	ICOSLG
DC	BATF3
mmune Cell Adhesion & Migration	PECAM1
T cells;T cell Activation	CD27
Th cells	TBX21
Tumor	PTEN
Checkpoint	CD276
T cells;Th cells;T cell Activation;Checkpoint	CTLA4
Myeloid Activation;Macrophage;Myeloid;Checkpoint	VSIR
Macrophage	CD68
Background	NegPrb4
Background	NegPrb6
Cytokine & Chemokine Signaling	CMKLR1
Cytokine & Chemokine Signaling	CXCL10
T cells;Th cells;Tregs	FOXP3
Immune Cell Adhesion & Migration	ITGAX
Antigen Presentation	HLA-E
Immune Cell Adhesion & Migration	ITGAM
Interferon	IFNAR1
Antigen Presentation;MHC2	HLA-DRB
Cytokine & Chemokine Signaling	CCL5
Background	NegPrb5
T cells	CD40LG
Wnt Signaling	DKK2
Immune Cell Adhesion & Migration	ITGB8
Epithelial;Tumor	EPCAM
Reference Gene	SDHA
Apoptosis;Cytokine & Chemokine Signaling	FAS
Antigen Presentation	PSMB10
T cell Activation;Cytotoxicity	GZMB
T cells;T cell Activation	TNFRSF9
Immune Cell Adhesion & Migration	ITGB2
Tumor;Wnt Signaling	CTNNB1
Apoptosis;Cytokine & Chemokine Signaling	TNF
Reference Gene	POLR2A
Cytokine & Chemokine Signaling	IL15
T cells	CD3E
Antigen Presentation;Tumor	B2M
T cells;Th cells;Myeloid	CD4
T cells;T cell Activation;Checkpoint	HAVCR2
Cytotoxicity	NKG7
Cytokine & Chemokine Signaling	STAT2
Tumor	AKT1
Tumor;Cytokine & Chemokine Signaling	HIF1A
Cytokine & Chemokine Signaling	IL12B
Total Immune	PTPRC
Reference Gene	UBB
T cell Activation	CD44
Antigen Presentation;MHC2	HLA-DQ
Cytokine & Chemokine Signaling	CXCL9
Cytokine & Chemokine Signaling	VEGFA
Proliferation	MKI67
Reference Gene	OAZ1
Myeloid Activation;Macrophage;M2 Macrophage; Myeloid;Myeloid Supression	ARG1
T cells;Checkpoint	TIGIT
T cells;T cell Activation;Checkpoint	PDCD1
T cells;T cell Activation;Checkpoint	LAG3
Reference Gene	RAB7A
Immune Cell Adhesion & Migration	ICAM1
Apoptosis;Tumour	BCL2
Checkpoint	PDCD1LG2
T cells;Myeloid	LY6E
Interferon	IFNGR1
Epithelial;Tumor	KRT
Interferon	IFNG

categorical variables. Recurrence free survival (RFS), disease-free survival (DFS) and overall survival (OS) curves were calculated with the Kaplan-Meier method and compared by the log-rank test. The Cox proportional hazards regression model with forward stepwise variable selection was used for multivariate analysis. A 2-tailed P-value less than 0.05 was considered statistically significant. Statistical analyses were performed using IBM SPSS software v. 28 (SPSS Inc., Chicago, IL, USA).

GeoMx digital spatial profiling

Preparation of slides

Sections from the TNBC TMA were cut at 2.5 µm and baked for 30 minutes at 60°C. The Leica BOND autostainer was employed to perform epitope retrieval (ER2, pH 9, 100°C) for 10 minutes and protein digestion using proteinase K (0.1 µg/ml) for 15 minutes. The slides were then stored until required in 1x PBS.

In situ hybridization of RNA-directed DNA oligo probes (Immune Pathways Panel, Nanostring) was performed as per manufacturer's protocol and added to each slide. HybriSlip™ covers were applied prior to overnight incubation at 37°C for at least 16 hours (Thermo fisher). The following day, once coverslips were removed, slides were washed twice with a 1:1 ratio of 100% deionized formamide (Ambion) and 4x SSC (Sigma Aldrich) at 37°C for 25 minutes. Immunofluorescence staining was performed using primary conjugated antibodies (PanCK, and CD45) and nucleic acid dye (SYTO13) for 1 hour as per manufacturers protocol. Slides were then stored at 4°C for up to 6 hours in 2x SSC before being loaded on the GeoMx DSP instrument for region selection and collection (Fig. 2).

Region of interest selection (ROI)

TMA cores from 52 patients, two cores per patient, were then selected for future analysis based on successful 3-plex immunofluorescence staining of SYTO 13, PanCK and CD45 to obtain regions of interest. Circular ROIs (0.6 mm) were selected on the basis of fluorescently labelled anti-PanCK (Fig. 3). PanCK+ used to select tumour-rich regions that were enriched for PanCK, and PanCK- to identify stroma-rich regions that were enriched for CD45 and lacked PanCK staining. After ROIs were selected, the GeoMx platform employs an automatically controlled UV laser to illuminate each ROI in turn, specifically cleaving barcodes within the ROI but not in surrounding tissue. A microcapillary collection system collected the liberated barcodes from each region and plated them into an individual well on a microtiter plate. This process was repeated in turn for each ROI before processing using

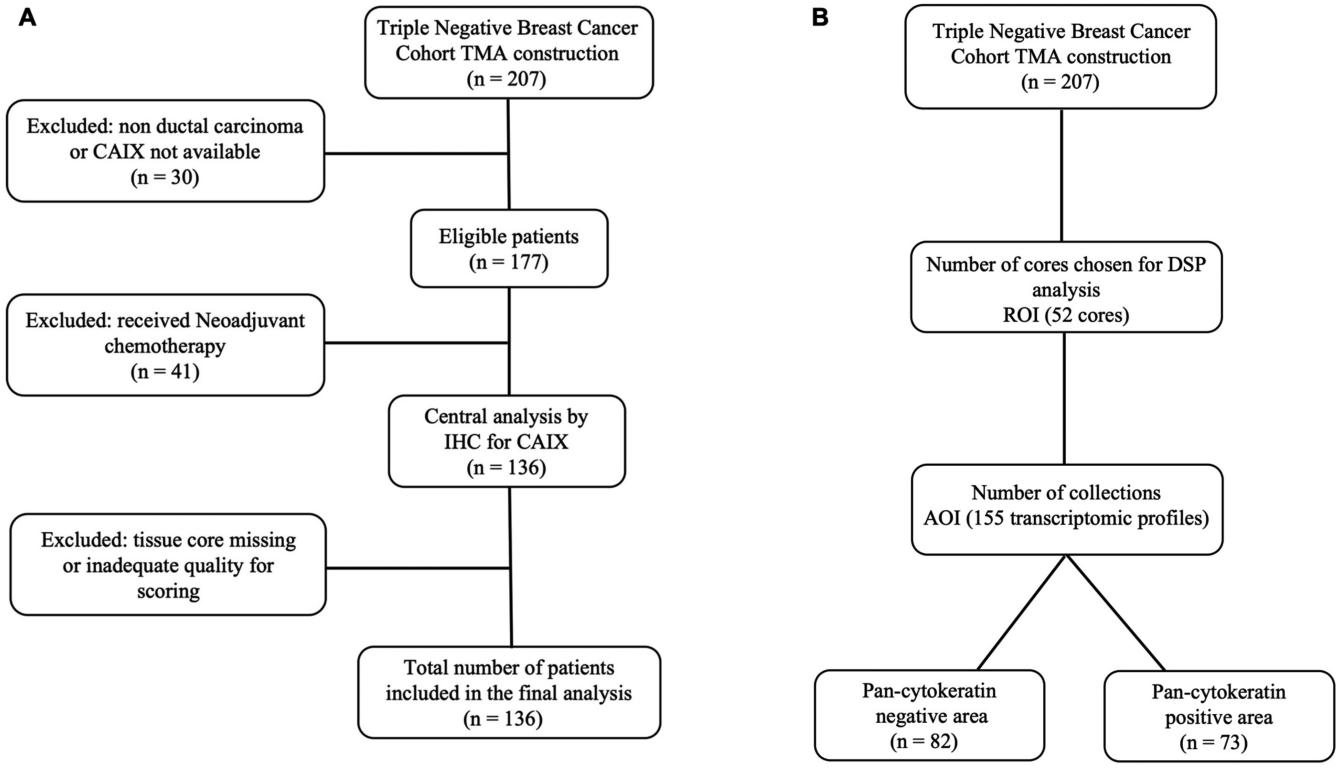

Fig. 1. CONSORT diagram in TNBC cohort. Patient exclusion criteria showing total number of patients included in IHC analysis **(A)**, Flow chart showing selection of 155 readouts for GeoMx analysis **(B)**.

Nanostring MAX/FLEX nCounter system.

nCounter hybridization assay for photocleaved oligo counting

nCounter readout of GeoMx DSP-collected probes was performed according to manufacturer's protocol (Nanostring, MAN-10089-08). In brief, samples were resuspended in dH_2O prior overnight incubation (16-24 hours) with hybridisation codes (Hyb Codes) at 65°C and heated lid (70°C). These Hyb Codes include reporter and capture probes to enable formation of a tripartite hybridization complex with the DNO oligo probes in the panel. Samples were then pooled by column into 12-well strip tube before processing on Nanostring's MAX/FLEX system, using the high sensitivity protocol (Nanostring, MAN-10089-08). Data acquisition was performed by using the Nanostring's Digital Analyser (FOV, 555).

GeoMx data analysis

GeoMx DSP analysis suite was used to perform preliminary analysis and QC (quality control) checks on transcriptomic data follow quantification by Nanostring's nCounter system. Using the GeoMx data analysis suite, the sequenced data underwent technical QC to exclude regions with suboptimal binding density (<0.1, >2.25) and/or high positive control normalisation (>3). Most correlated normalisation method was used following assessment using custom script. The counts also underwent normalisation with negative probes using the geometric mean. Data analysis was performed to identify differences in gene expression between high CAIX tumours versus low CAIX tumours. Differential gene expression was performed using the GeoMx analysis suite, which utilises the GeoMxTools R package

Table 3. Clinicopathological characteristics of TNBC patients (n=136).

Clinicopathological characteristics	Patients, n (%)
Age (≤ 50/>50 years)	36(26)/100(74)
Size (≤ 20/21-50/>50mm)	60(45)/68(51)/6(4)
Grade (I/II/III)	0(0)/5(4)/131(96)
Lymph node status (negative/positive)	104(78)/30(22)
Chemotherapy (no/yes)	44(32)/92(68)
Radiotherapy (no/yes)	34(25)/102(75)
Alive/cancer death/non-cancer death	95(70)/33(24)/8(6)
Alive with no recurrence/recurrence/bilateral	101(76)/30(22)/3(2)

Table 4. Relationship between cytoplasmic CAIX expression and clinicopathological characteristics in TNBC cohort (n=136).

Clinicopathological characteristics	Cytoplasmic CAIX		
	Low 102 (75%)	High 34 (25%)	P-value
Age (≤50/>50 years)	28(27)/74(73)	8(23)/26(77)	0.651
Tumour size (≤20/21-50/>50 mm)	48(48)/47(47)/6(5)	12(36)/21(64)/0(0)	0.652
Grade (I/II/III)	0(0)/4(4)/98(96)	1(3)/33(97)	0.793
Involved lymph node (negative/positive)	78(78)/22(22)	26(77)/8(23)	0.854
Lymphatic vessel invasion (no/yes)	11(11)/88(90)	4(13)/27(87)	0.788
Blood vessel invasion (no/yes)	64(63)/37(37)	26(77)/8(23)	0.152
Tumour necrosis (low/high)	46(46)/54(54)	14(45)/17(55)	0.935
Klintrup-Mäkinen grade (low/high)	13(13)/39(40)/32(33)/14(14)	4(13)/14(47)/9(30)/3(10)	0.541
Tumour stroma percentage (low/high)	69(70)/30(30)	22(71)/9(29)	0.893
Adjuvant chemotherapy (no/yes)	31(30)/71(70)	13(38)/21(62)	0.402
Adjuvant radiotherapy (no/yes)	18(18)/84(82)	16(47)/18(53)	<0.001

Table 5. Univariate and multivariate analysis for recurrence free survival of CAIX and clinicopathological characteristics in TNBC (n=136).

Clinicopathological characteristics	Univariate analysis		Multivariate analysis	
	HR (95%CI)	P-value	HR (95%CI)	P-value
Age (≤50/>50years)	4.11 (0.51-33.15)	0.184	-	-
Tumour size (≤ 20/21-50/>50 mm)	3.49 (1.12-10.89)	0.032	3.92 (0.92-16.62)	0.064
Grade (I / II / III)	0.32 (0.04-2.59)	0.287	-	-
Lymph node (negative/positive)	3.49 (0.93-13.07)	0.063	-	-
Lymphatic vessel invasion (no/yes)	1.32 (0.33-5.28)	0.696	-	-
Blood vessel invasion (no/yes)	1.32 (0.33-5.28)	0.696	-	-
Tumour necrosis (low/high)	0.56 (0.14-2.25)	0.416	-	-
Klintrup-Mäkinen grade (low/high)	0.27 (0.09-0.75)	0.012	0.26 (0.09-0.74)	0.012
Tumour stroma percentage (low/high)	1.52 (0.36-6.35)	0.570	-	-
Adjuvant chemotherapy (no/yes)	0.37 (0.09-1.38)	0.137	-	-
Adjuvant radiotherapy (no/yes)	0.27 (0.07-1.02)	0.053	-	-
Cytoplasmic CAIX (low/high)	3.67 (0.98-13.69)	0.038	6.59 (1.47-29.58)	0.014

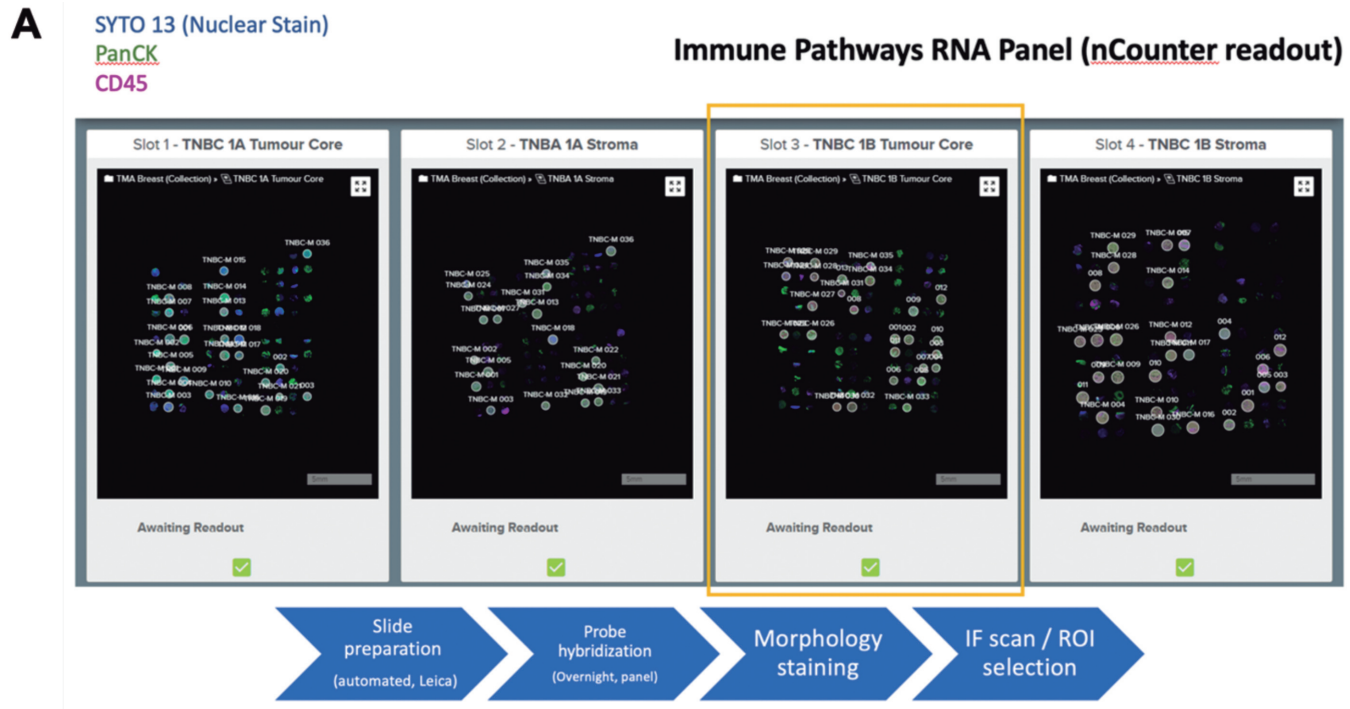

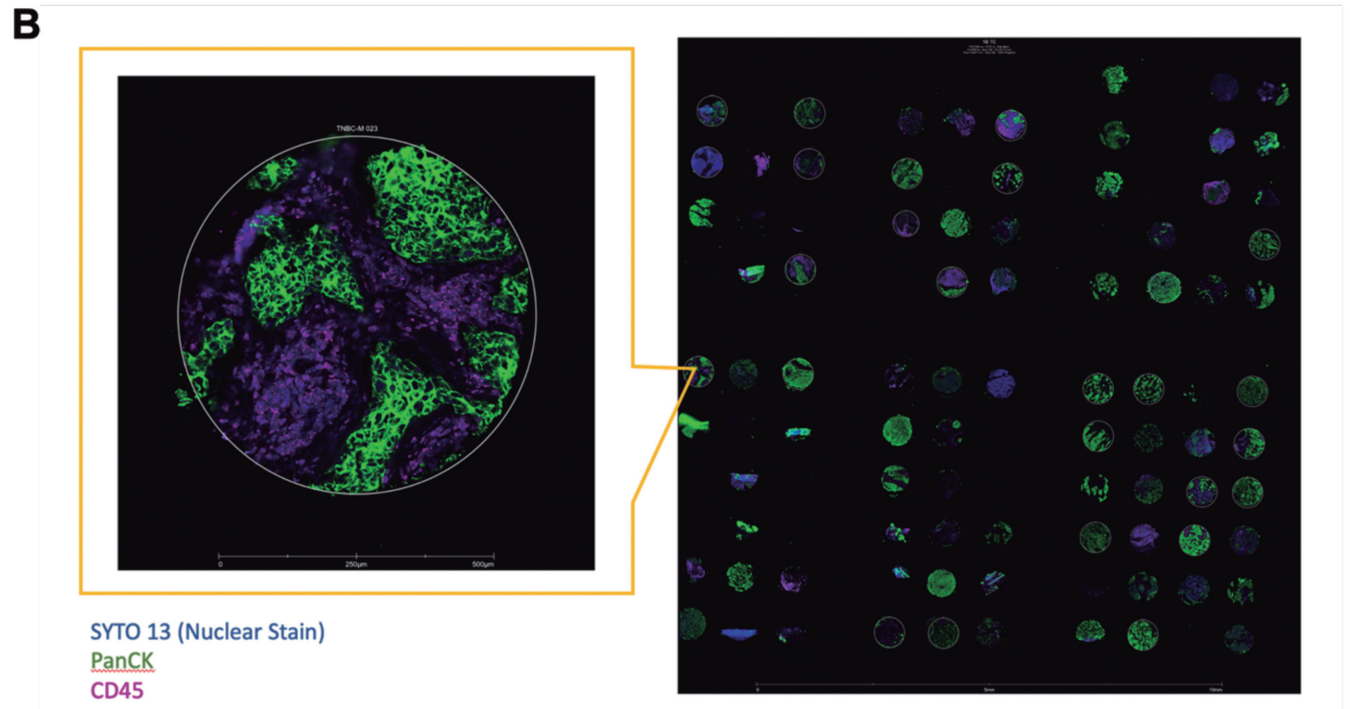

Fig 2. Region of interest selection in TNBC. The picture showed the GeoMx suit where region of interested (ROI) has been selected **(A)**, The tissue morphology was delineated by the immunofluorescence detection of PanCK (epithelial cytokeratin, green), CD45+ (immune cells, magenta) proteins and SYTO13 (nuclei, blue) **(B)**.

(tool: 'mixedModelDE' in R package 'lmerTest'). Volcano plots were created using a plugin script, available at: (https://github.com/NanostringBiostats/DSPPlugins/tree/master/DSPPlugVolcanoPlot). Heatmaps were created using negative probe-normalised counts as input to R package, Complexheatmap (RStudio, Boston, MA, USA). The differentially expressed genes (DEGs) screened out with the criteria of log2 fold change (FC)>(±0.25 and ±0.3) for tumour and stromal compartment, respectively, and P-value <0.05. The number of genes assessed in the RNA panel was 84 genes (Table 2).

Results

Patient characteristics

Clinicopathological characteristics and survival status of selected patients (n=136) are summarized in Table 3. The majority of patients were over 50 years of age (74%), had tumour size 21-50 (51%), had grade III carcinoma (96%), and had negative lymph nodes (78%). 92 (68%) patients received chemotherapy and 102 (75%) received radiotherapy. One hundred one patients (76%) had no recurrence, and thirty-three patients (24%) experienced recurrences. Of these patients, 3 (2%) had bilateral recurrence. The follow up for the patients ranged from 0-112 months and a median follow up time was 54 months (range 38.75-68.68 months) with 33 cancer-associated deaths and 8 non-cancer deaths.

Levels of CAIX expression and its relation to clinicopathological variables

CAIX immunoreactivity was readily detected in the cytomembrane of tumour cells. Representative images for CAIX are presented in Fig. 4A,B. A correlation coefficient of 0.942, and 0.864 for cytoplasmic and

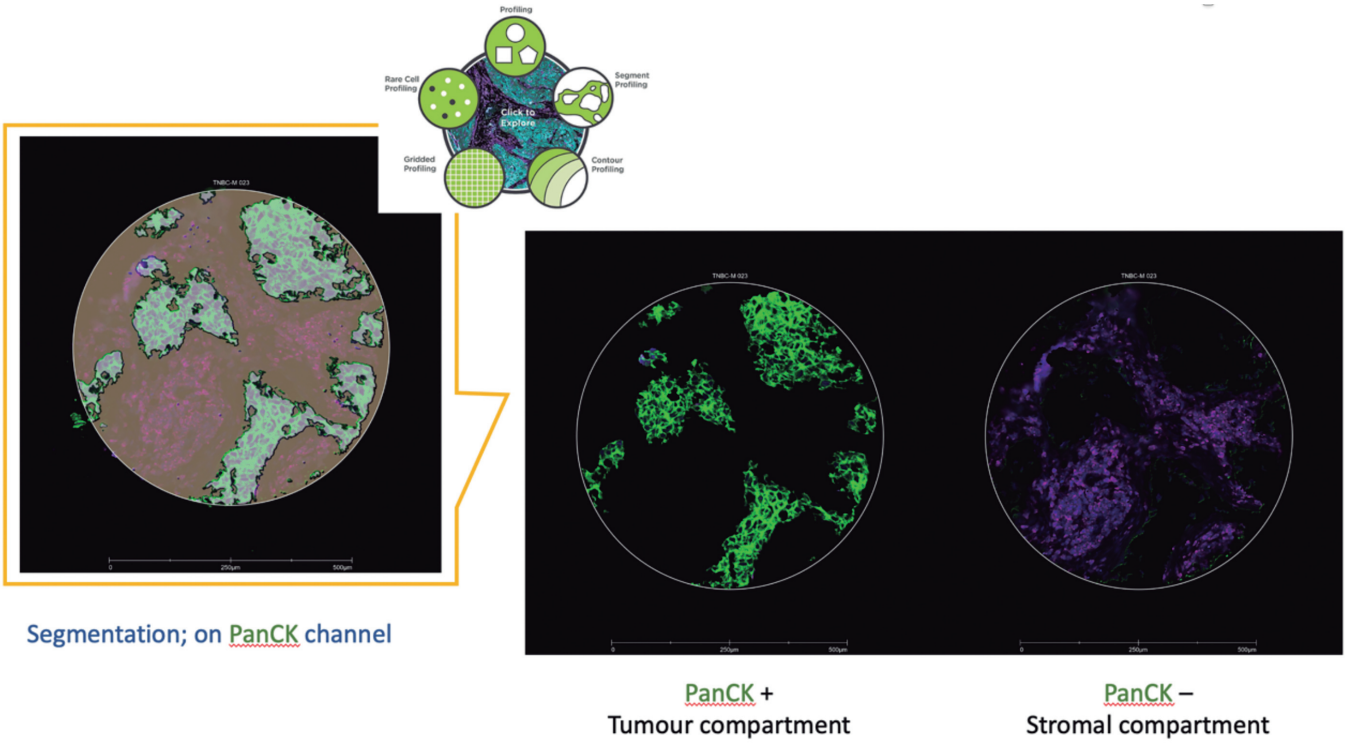

Fig 3. The images segmentation according to the PanCK mask selected by Geometric. PanCK+ for tumour compartment, PanCK- for stromal compartment.

Table 6. The significant genes comparing high and low cytoplasmic CAIX expression in pan-cytokeratin positive group.

Target name	Description	Categories	Log2 FC	P-value
CD68	CD68 Molecule	Macrophage	- 0.371574835	0.008896029
HIF1A	Hypoxia Inducible Factor 1 Subunit Alfa	Tumour, cytokine, and chemokine signalling	- 0.274447855	0.011833749
pan-melanocyte	Pan-melanocyte	Melanoma	0.245326804	0.016388306
VSIR	V-Set Immunoregulatory Receptor	Myeloid activation, macrophage, myeloid checkpoint	- 0.097641803	0.029824509

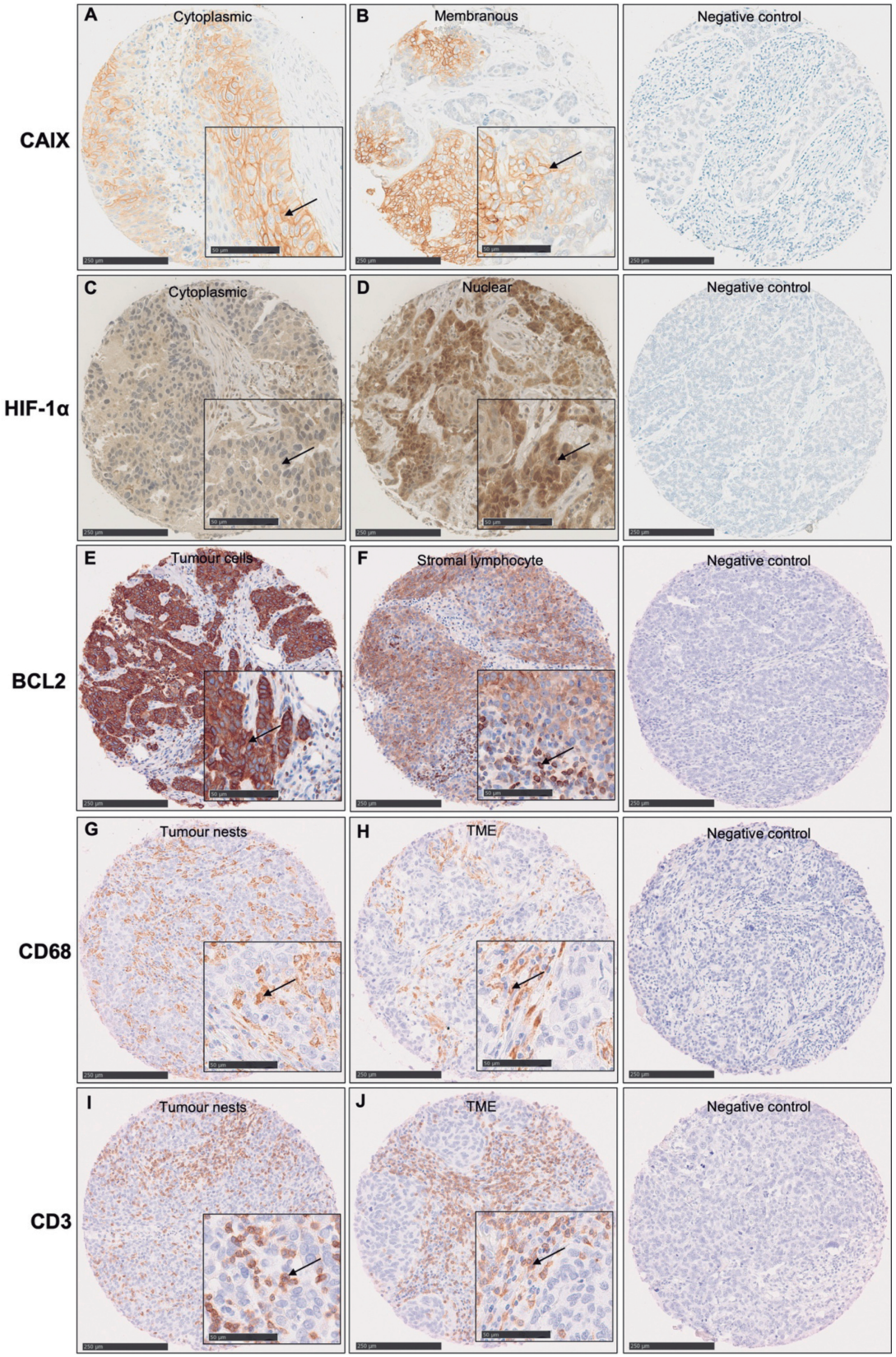

Fig. 4. Representative images of immunohistochemistry staining of examined markers in TNBC samples. Cytoplasmic and membranous CAIX expression **(A, B)**, cytoplasmic and nuclear HIF-1α expression **(C, D)**, cytoplasmic BCL2 expression in tumour cells and immune cells and (arrows) **(E, F)**, cytoplasmic CD68 are noted in tumour nests and TME (arrows) **(G, H)**, cytoplasmic CD3 infiltration of both tumour nests and TME (arrows) **(I, J)**. No negative control antibody was used in the breast cancer TMA to rule out nonspecific staining in the last column. Scale bars: 250 μm.

membranous CAIX was obtained between the 2 estimations. Chi-square analysis showed an association between cytoplasmic CAIX expression and patients who received radiotherapy (P<0.001) (Table 4), but no other associations were found.

Association of the CAIX protein level with the survival of TNBC patients

TNBC patients that had high cytoplasmic expression of CAIX had lower RFS (log-rank, P=0.038) while no association with DFS and OS was found (Fig. 5). In contrast, there was no significant association with patients' survival in membranous expression. When multivariate analysis was performed, cytoplasmic CAIX remained as a factor contributing significantly to RFS (HR=6.59, 95% CI: 1.47-29.58, P=0.014) for TNBC patients along with tumour size, and KM grade (Table 5).

GeoMx digital spatial profiling

To determine the correlation of gene expression data with high and low cytoplasmic CAIX expression within PanCK+ (tumour epithelium) and PanCK- (tumour microenvironment) samples, the GeoMx DSP was used. DEGs were identified in a comparison of high and low CAIX expression groups by using the RStudio (RStudio, Boston, MA, USA).

Identification of DEGs with cytoplasmic CAIX expression in tumour compartment

The DEGs were filtered according to log2 FC>(±0.25 and ±0.3) and P<0.05, then, volcano plot was constructed. Within PanCK+ compartment (tumour-rich region), high cytoplasmic CAIX expression group had significantly higher expression of three genes, including CD68, HIF1A, VSIR, and lower expression of one gene, pan-melanocyte (Table 6). Volcano plot was plotted to visualize the FC and determine the statistically significance differences between the high and low cytoplasmic CAIX expression groups (Fig. 6A). In addition, within PanCK+ compartment, the heatmap with clustering for the significantly differentially expressed genes between high and low cytoplasmic CAIX expression groups were generated using the ggplot package. There was no clear pattern associated with CAIX expression levels (Fig. 6B).

Identification of DEGs with cytoplasmic CAIX expression in stromal compartment

Based on stromal compartment (PanCK- segments), low cytoplasmic CAIX expression had significantly higher expression of 8 genes, including CD86, CD3E, MS4A1, BCL2, CCL5, NKG7, PTPRC and CD27 (Table 7). Genes were ordered by P-value, regardless of log2 FC. Volcano plot was used to determine the statistically significance differences between the high and low cytoplasmic CAIX expression groups (Fig. 7A). Correspondingly, for grouping comparisons based on the CAIX expression in PanCK-, the heatmap demonstrated noticeable gene expression differences when the high CAIX expression group was compared to the low expression group. Most of high expression genes were

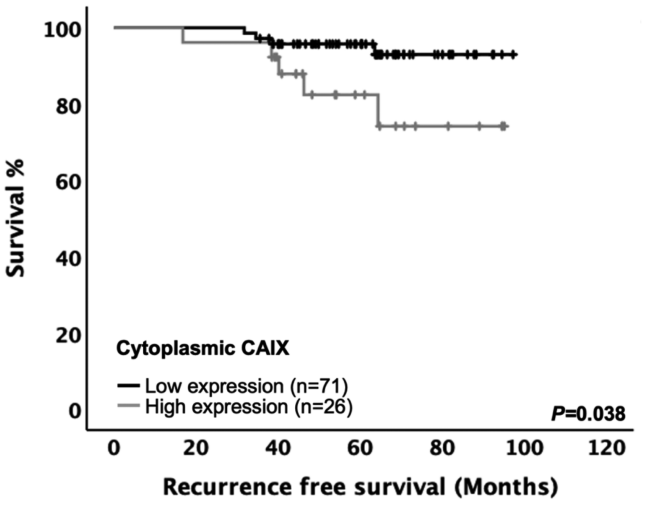

Fig. 5. Expression of CAIX and clinical outcome in triple negative breast cancer. Kaplan-Meier curves showing an association between cytoplasmic CAIX with RFS.

Table 7. The significant genes comparing low and high cytoplasmic CAIX expression in pan-cytokeratin negative group.

Target name	Description	Categories	Log2 FC	P-value
CD86	CD86 Molecule	T cell activation, myeloid checkpoint	0.194619932	0.000425023
CD3E	CD3e Molecule	T cells	0.300552796	0.005474011
MS4A1	Membrane Spanning 4-Domains A1	B cells	0.22399975	0.007014351
BCL2	B-cell lymphoma-2	Apoptosis	0.194899023	0.008449576
CCL5	C-C Motif Chemokine Ligand 5	Cytokine and chemokine signalling	0.35022514	0.012321049
NKG7	Natural Killer cell Granule protein 7	Cytotoxicity	0.19508988	0.024832855
PTPRC	Protein Tyrosine Phosphatase Receptor Type C	Total immune	0.32467447	0.035836939
CD27	CD27 Molecule	T cells	0.169683196	0.041806309
FAS	Cell Surface Death Receptor	Apoptosis, cytokine, and chemokine signalling	0.119141511	0.053309814

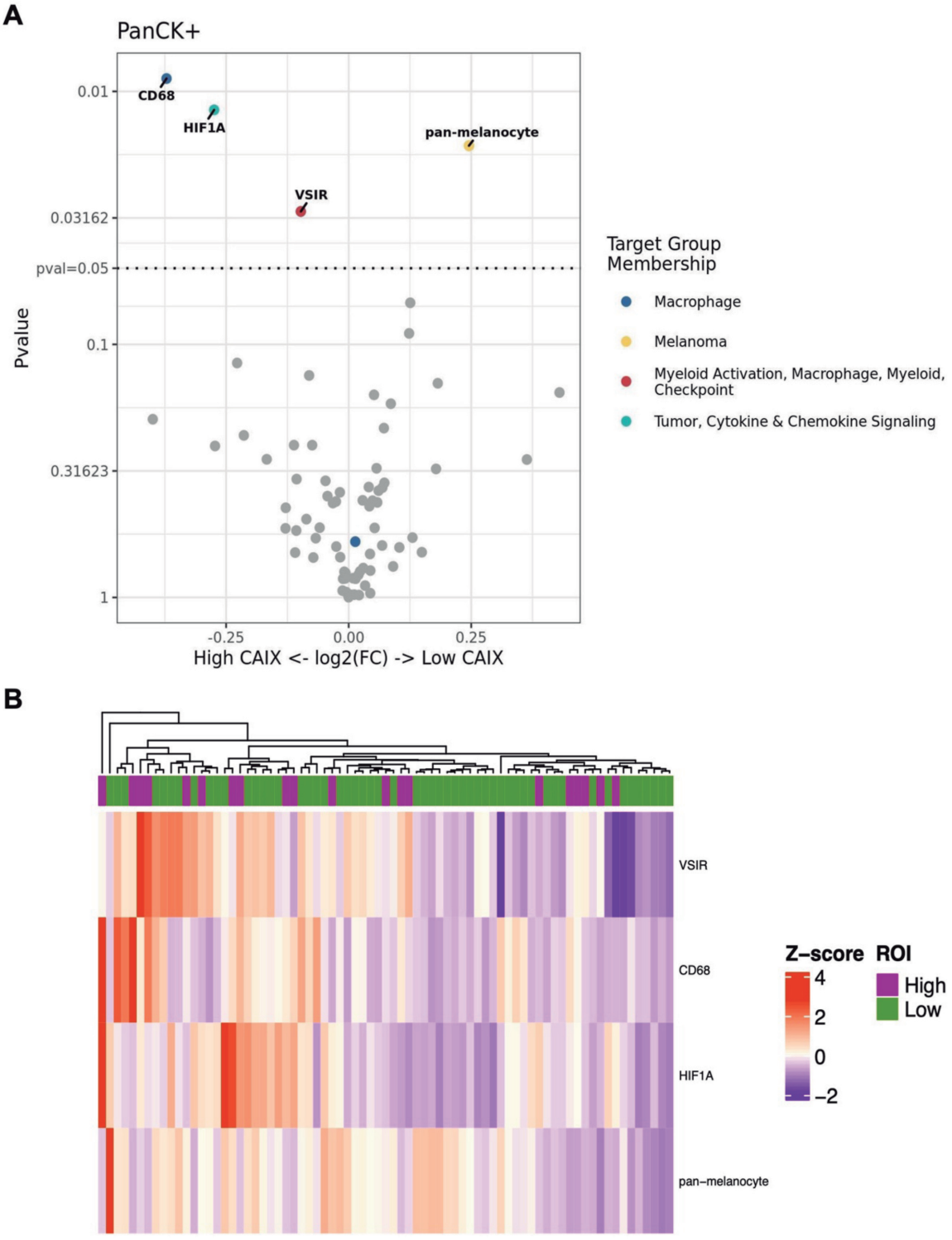

Fig. 6. Volcano plot and heatmap of differentially expressed genes in PanCK+ tumour with high and low cytoplasmic CAIX expression groups. Volcano plot of DEGs in PanCK+ describes log2 FC in the X-axis and P-value in the Y-axis. The line parallel to the X-axis represents a value of P=0.05. P-value<0.05 was considered significant **(A)**, Hierarchical clustering analysis and heatmap of the DEGs in PanCK+ tumour. Each row represents a single gene and each column represent a tumour sample. The scale bar shows the relative gene expression levels corresponding to the colours in the heatmap. As shown in the colour bar, orange indicates up regulation and purple represents down regulation **(B)**.

shown in low CAIX expression group as shown in Fig. 7B.

Validation of the identified genes in the tissue microarray TNBC samples

To evaluate the significance of the four selected genes HIF1A, BCL2, CD68, and CD3, their expression patterns in TNBC datasets were validated by IHC at protein level with respect to hypoxic marker CAIX. Most of the proteins selected to study in this work have a well-established role in BC prognosis (Bouchalova et al., 2014; Rathore et al., 2014; Ni et al., 2019; Shamis et al., 2021). In addition, antibodies are in routine clinical use in pathology laboratories.

Levels of HIF-1α, BCL2, CD68 and CD3 expression and their relation to clinicopathological variables

The staining pattern for HIF-1α was cytoplasmic and nuclear as observed in TNBC cores (Fig. 4C,D). There was good correlation between observers for cytoplasmic and nuclear HIF-1α with an ICCC score of 0.887 and 0.827, respectively. 20 of 133 (15%) tumours were designated as having high cytoplasmic HIF-1α expression and 102/133 samples (75%) had high nuclear HIF-1α expression (Table 8). High nuclear HIF-1α expression was significantly associated with lymph node negativity and tumour necrosis (P=0.035, 0.011, respectively) (Table 9). No significant correlation was found between the cytoplasmic HIF-1α status and clinicopathological variables.

Immunohistochemical expression of BCL2 was found in the cytoplasm of tumour cells and stromal lymphocyte as illustrated in Figure 4E,F. Excellent ICCC of 0.937 was found between two observers with 26 of 130 (20%) tumours were scored as high cytoplasmic BCL2 within stromal cells. BCL2 positive staining was correlated with lymph node negativity (P=0.003), tumour necrosis (P=0.048), and being mainly expressed in tumour samples of patients who received adjuvant radiotherapy (P=0.033) (Table 10).

Immunostaining showed a cytoplasmic staining of CD68 in both tumour nests and TME (Fig. 4G,H). A correlation coefficient of 0.888 and 0.910 was obtained between two observers for CD68 scoring in tumour nests and TME respectively. 81 of 128 (63%) tumours showed high CD68 number in tumour nests. 95 of 128 (74%) samples showed high CD68 number in TME, and 103 of 128 (81%) tumours showed high total CD68 immunoreactivity (Table 8). Higher TME CD68 counts were associated with lymphatic vessel invasion and tumour necrosis (P=0.007, 0.033, respectively), while higher total CD68 was associated with high tumour grade (P=0.025) (Table 11).

Similarly, CD3-positive staining showed cytoplasmic staining within both tumour nests and TME (Fig. 4I,J). Excellent ICCC of 0.989, 0.984 and 0.983

Table 8. Protein markers expression in a total of 136 TNBC patients.

Markers		Cytoplasmic n (%)	Nuclear n (%)	Missing cases n (%)
HIF-1α	Low	113 (85)	31 (23)	3 (2)
	High	20 (15)	102 (77)	
BCL2	Low	26 (20)	-	6 (4)
	High	104 (80)		
CD68				
Tumour nests	Low	47 (37)	-	8 (6)
	High	81 (63)		
TME	Low	33 (26)	-	8 (6)
	High	95 (74)		
Total	Low	25 (19)	-	8 (6)
	High	103 (81)		
CD3				
Tumour nests	Low	13 (10)	-	1 (0.7)
	High	122 (90)		
TME	Low	21 (16)	-	1 (0.7)
	High	114 (84)		
Total	Low	13 (10)	-	1 (0.7)
	High	115 (90)		

Table 9. Relationship between nuclear HIF-1α expression and clinicopathological characteristics in TNBC cohort (n=136).

Clinicopathological characteristics	Nuclear HIF-1α		
	Low 31 (23%)	High 102 (77%)	*P*-value
Age (≤50/>50 years)	8(26)/23(74)	27(26)/75(74)	0.941
Tumour size (≤ 20/21-50/>50 mm)	14(47)/15(50)/1(3)	45(44)/52(52)/4(4)	0.816
Grade (I/II/III)	2(6)/29(94)	3(3)/99(97)	0.397
Lymph node (negative/positive)	20(65)/11(35)	83(83)/17(17)	0.035
Lymphatic vessel invasion (no/yes)	3(10)/27(90)	11(11)/86(89)	0.836
Blood vessel invasion (no/yes)	22(71)/9(29)	66(65)/35(35)	0.558
Tumour necrosis (low/high)	8(26)/23(74)	50(51)/47(49)	0.011
Klintrup-Mäkinen grade (0/1/2/3)	3(11)/11(39)/9(32)/5(18)	13(13)/41(42)/32(33)/11(12)	0.428
Tumour stroma percentage (low/high)	25(83)/5(17)	65(67)/32(33)	0.074
Adjuvant chemotherapy (no/yes)	7(23)/24(77)	36(35)/66(65)	0.175
Adjuvant radiotherapy (no/yes)	5(16)/26(84)	29(28)/73(72)	0.154

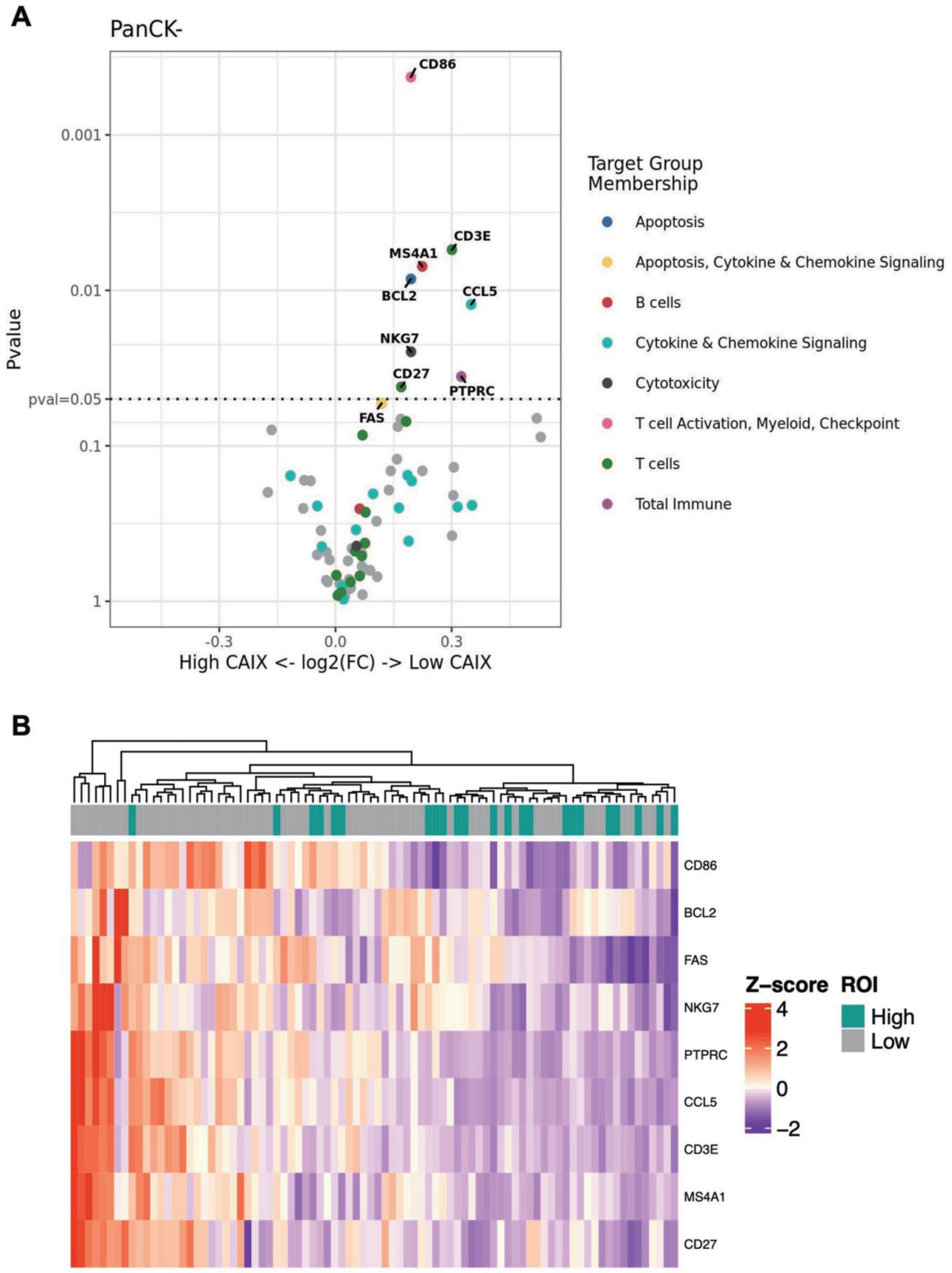

Fig. 7. Volcano plot and heatmap of differentially expressed genes in PanCK- tumour with high and low cytoplasmic CAIX expression groups. Volcano plot of DEGs in PanCK- describes log2 FC in the X-axis and P-value in the Y-axis. The line parallel to the X-axis represents a value of P=0.05. P-value<0.05 was considered significant **(A)**, Hierarchical clustering analysis and heatmap of the DEGs in PanCK- tumour. Each row represents a single gene and each column represent a tumour sample. The scale bar shows the relative gene expression levels corresponding to the colours in the heatmap. As shown in the colour bar, orange indicates up regulation and purple represents down regulation **(B)**.

was found for CD3 in tumour nests, TME and total CD3, respectively between two observers. As shown in Table 8, IHC staining showed high CD3 density in 122 of 135 samples (90%) in tumour nests, 114 of 135 (84%) in TME, and 115 of 128 (90%) samples of total CD3 density in TNBC. There was also a significant association between the numbers of CD3 in TME and KM grade (P=0.005) (Table 12).

Association of CAIX tumour expression with the four markers

In Chi-square analysis, the IHC CAIX protein level of the tumour cells was correlated, as expected, with the IHC HIF-1α protein expression (P=0.010) in the same tumour samples. CAIX protein expression was also associated positively with high CD68 cells number in

Table 10. Relationship between BCL2 expression and clinicopathological characteristics in TNBC cohort (n=136).

Clinicopathological characteristics	Cytoplasmic BCL2		
	Low 26 (20%)	High 104 (80%)	P-value
Age (≤50/>50 years)	5(19)/21(81)	31(30)/73(70)	0.267
Tumour size (≤ 20/21-50/>50 mm)	10(38)/16(62)/0(0)	46(45)/51(50)/5(5)	0.889
Grade (I/II/III)	1(4)/25(96)	2(2)/102(98)	0.584
Lymph node (negative/positive)	25(96)/1(4)	74(73)/28(27)	0.003
Lymphatic vessel invasion (no/yes)	4(16)/21(84)	11(11)/88(89)	0.516
Blood vessel invasion (no/yes)	18(69)/8(31)	69(67)/34(33)	0.827
Tumour necrosis (low/high)	16(64)/9(36)	42(42)/58(58)	0.048
Klintrup-Mäkinen grade (0/1/2/3)	5(20)/11(44)/9(36)/0(0)	12(12)/39(40)/31(32)/15(16)	0.081
Tumour stroma percentage (low/high)	16(64)/9(36)	72(73)/27(27)	0.398
Adjuvant chemotherapy (no/yes)	12(46)/14(54)	30(29)/74(71)	0.098
Adjuvant radiotherapy (no/yes)	11(42)/15(58)	22(21)/82(79)	0.033

Table 11. Relationship between CD68 expression and clinicopathological characteristics in TNBC cohort (n = 136)

Clinicopathological characteristics	TME CD68			Total CD68		
	Low 33 (26%)	High 95 (74%)	P-value	Low 13 (10%)	High 115 (90%)	P-value
Age (≤50/>50 years)	10(30)/23(70)	22(23)/73(77)	0.420	2(15)/11(85)	30(26)/85(74)	0.376
Tumour size (≤ 20/21-50/>50 mm)	17(52)/16(48)/0(0)	39(42)/48(52)6(6)	0.173	8(62)/5(38)/0(0)	48(43)/59(52)/6(5)	0.152
Grade (I/II/III)	0(0)/2(6)/31(94)	0(0)/3(3)92(97)	0.460	0(0)/2(15)/11(85)	0(0)/3(3)/112(97)	0.025
Lymph node (negative/positive)	25(76)/8(24)	74(80)/19(20)	0.650	11(85)/2(15)	88(78)/25(22)	0.561
Lymphatic vessel invasion (no/yes)	8(26)/23(74)	6(7)/85(93)	0.007	3(23)/10(77)	11(10)/98(90)	0.207
Blood vessel invasion (no/yes)	20(61)/13(39)	65(69)/29(31)	0.374	8(62)/5(38)	77(68)/37(32)	0.666
Tumour necrosis (low/high)	20(63)/12(37)	37(41)/54(59)	0.033	9(69)/4(31)	48(44)/62(56)	0.078
Klintrup-Mäkinen grade (0/1/2/3)	4(13)/17(57)/5(17)/4(13)	10(11)/34(38)/35(39)/11(12)	0.220	2(17)/7(58)/3(25)/0(0)	12(11)/44(41)/37(34)/15(14)	0.103
Tumour stroma percentage (low/high)	20(65)/11(35)	66(73)/25(27)	0.404	9(69)/4(31)	77(71)/32(29)	0.916
Adjuvant chemotherapy (no/yes)	9(27)/24(73)	33(35)/62(65)	0.426	4(31)/9(69)	38(33)/77(67)	0.868
Adjuvant radiotherapy (no/yes)	8(24)/25(76)	25(26)/70(74)	0.814	2(15)/11(85)	31(27)/84(73)	0.342

Table 12. Relationship between CD3 expression and clinicopathological characteristics in TNBC cohort (n=136).

Clinicopathological characteristics	TME CD3		
	Low 21 (16%)	High 114 (84%)	P-value
Age (≤50/>50 years)	5(24)/16(76)	31(27)/83(73)	0.745
Tumour size (≤ 20/21-50/>50 mm)	7(35)/13(65)/0(0)	52(46)/55(49)/6(5)	0.683
Grade (I/II/III)	0(0)/0(0)/21(100)	5(4)/109(96)	0.189
Lymph node (negative/positive)	15(71)/6(29)	88(79)/24(21)	0.482
Lymphatic vessel invasion (no/yes)	2(9)/19(91)	13(12)/95(88)	0.737
Blood vessel invasion (no/yes)	14(67)/7(33)	75(66)/38(34)	0.979
Tumour necrosis (low/high)	11(52)/10(48)	48(44)/61(56)	0.483
Klintrup-Mäkinen grade (0/1/2/3)	5(24)/13(62)/2(10)/1(4)	12(11)/40(38)/39(37)/15(14)	0.005
Tumour stroma percentage (low/high)	16(76)/5(24)	75(69)/33(31)	0.528
Adjuvant chemotherapy (no/yes)	7(33)/14(67)	37(32)/77(68)	0.937
Adjuvant radiotherapy (no/yes)	6(29)/15(71)	28(25)/86(75)	0.701

tumour nests (P=0.039) and negatively with BCL2 protein level (P=0.033). CAIX protein expression did not correlate with the CD3 marker (Table 13).

Prognostic values of individual markers

We next analysed the prognostic values of HIF-1α, BCL2, CD68, and CD3 in TNBC. At protein level, Kaplan-Meier plots indicated a strong association of high cytoplasmic HIF-1α with RFS (P=0.048) (Fig. 8A) but not with DFS and OS. Furthermore, Kaplan-Meier plots showed that patients with high nuclear HIF-1α expression had shorter DFS (P=0.003) and OS (P=0.016) (Fig. 8B,C). However, no significant difference in RFS was observed between low and high nuclear HIF-1α expression groups.

In addition, the patients with lower BCL2 expression levels had unfavourable outcomes compared to those with higher BCL2 expression level group by using Kaplan-Meier plotter analysis. Lower expression of BCL2 was associated with poorer RFS and DFS (P=0.001, 0.009, respectively) (Fig. 9A,B). No association was found with OS.

The prognostic significance of CD68 infiltration levels according to the different histologic locations was also investigated. Univariate Kaplan-Meier analysis and log-rank test showed that high density CD68 cells in tumour nests, TME, and total CD68 infiltration was correlated with lower DFS (P=0.049, 0.048, 0.039, respectively) (Fig. 10A-C). Similarly, a high density of CD68 cells in tumour nests, TME, and total CD68 was also associated with a lower OS (log-rank, P=0.043, 0.030, 0.018, respectively) (Fig. 10D-F). However, no correlation between CD68 cells and RFS was detected in this study.

Moreover, a low density of CD3 T cells in tumour nests, TME and total density was associated with a poorer RFS (log-rank, P=0.020, 0.002, 0.013, respectively) (Fig. 11A-C). However, CD3 infiltration levels did not predict DFS and OS in this study.

To examine the independent prognostic significance of clinicopathological variables and markers expression, multivariate analysis was performed. High density CD68 in tumour nests (HR=2.42, 95% CI: 1.05-5.59, P=0.038), and in TME (HR=3.34, 95% CI: 1.28-8.69, P=0.014) were factors of poorer OS along with tumour necrosis, and adjuvant radiotherapy (Table 14).

Discussion

Previously, the TMEs of BC were analysed using DSP, however focus was given to protein expression (Stewart et al., 2020). The present study combined proteomic and transcriptomic data on the same tissue section to investigate differential gene expression in tumour and stromal/immune cells with high and low CAIX expression. To best of our knowledge, this is the first such study in patients with TNBC in a broad tumour and immune context, therefore paving the way to the identification of reliable predictive biomarkers and design of innovative therapies when properly correlated with clinical outcomes. The transcriptomics provided markers, CD68, HIF-1α, CD3, and BCL2, for studying

Table 13. Chi-squared test showing the relationship between cytoplasmic CAIX expression and protein markers in TNBC patients (n=136).

Markers	Cytoplasmic CAIX
Cytoplasmic HIF-1α	0.010
Nuclear HIF-1α	0.355
Cytoplasmic BCL2	0.033
CD68 in tumour nests	0.039
CD68 in TME	0.728
Total CD68	0.865
CD3 in tumour nests	0.853
CD3 in TME	0.153
Total CD3	0.126

Table 14. Univariate and multivariate analysis for overall survival of protein markers and clinicopathological characteristics in TNBC (n=136).

Clinicopathological characteristics	Univariate analysis		Multivariate analysis	
	HR (95%CI)	P-value	HR (95%CI)	P-value
Age (≤50/ >50 years)	2.13 (0.94-4.81)	0.070	-	-
Tumour size (≤ 20/21-50/>50 mm)	2.07 (1.24-3.46)	0.005	1.01 (0.99-1.03)	0.562
Grade (I / II / III)	1.51 (0.21-10.97)	0.686	-	-
Lymph node (negative/positive)	1.38 (0.69-2.77)	0.363	-	-
Lymphatic vessel invasion (no/yes)	1.24 (0.44-3.49)	0.686	-	-
Blood vessel invasion (no/yes)	1.68 (0.91-3.12)	0.099	-	-
Tumour necrosis (low/high)	0.386 (0.19-0.75)	0.005	0.41 (0.19-0.84)	0.016
Klintrup-Mäkinen grade (low/high)	0.87 (0.61-1.24)	0.443	-	-
Tumour stroma percentage (low/high)	1.29 (0.67-2.49)	0.442	-	-
Adjuvant chemotherapy (no/yes)	0.37 (0.20-0.68)	0.001	0.67 (0.31-1.45)	0.308
Adjuvant radiotherapy (no/yes)	0.45 (0.24-0.85)	0.014	0.39 (0.20-0.78)	0.007
Nuclear HIF-1α (low/high)	3.83 (1.17-12.45)	0.026	3.01 (0.91-10.01)	0.072
CD68 in tumour nests (low/high)	2.19 (1.01-4.79)	0.049	2.42 (1.05-5.59)	0.038
CD68 in TME (low/high)	2.72 (1.06-6.99)	0.037	3.34 (1.28-8.69)	0.014
Total CD68 (low/high)	24.93 (0.38-1629.6)	0.132	-	-

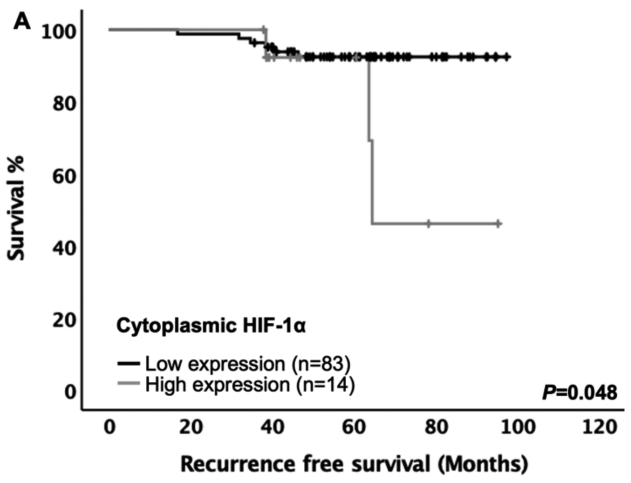

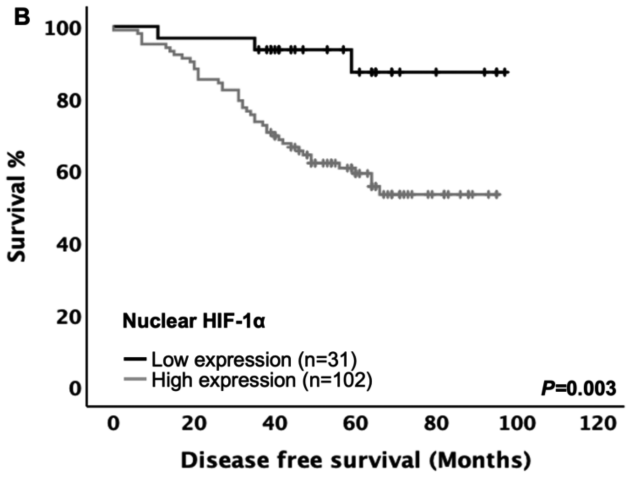

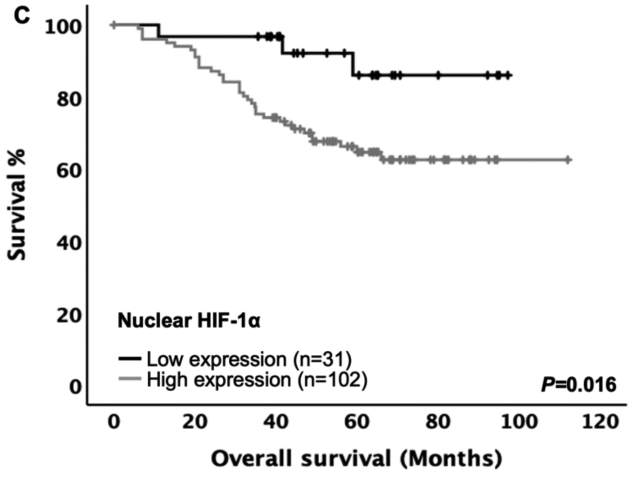

Fig. 8. Expression of HIF-1α and clinical outcome in triple negative breast cancer. Kaplan-Meier curves showing associations of cytoplasmic HIF-1α with recurrence free survival **(A)**, and nuclear HIF-1α with disease-free survival **(B)**, and overall survival **(C)**.

by IHC, and these are markers already employed in breast cancer.

Preliminary data compared high and low CAIX expression in pan-cytokeratin rich regions identified four genes: CD68, HIF-1α, pan-melanocyte and VSIR. Three genes were significantly down-regulated, and one was up-regulated in the low CAIX expression group. In contrast, GeoMx analysis of RNA expression within PanCK-negative samples identified significant 8 up-regulated microenvironment-related genes, CD86, CD3E, MS4A1, BCL2, CCL5, NKG7, PTPRC, CD27, and FAS with low compared to high CAIX expression groups. These common genes are signatures of stromal and immune cells, which play critical roles in the TME.

CD68 mRNA was up-regulated with high CAIX expression (log2 FC-0.372, P=0.009). CD68 gene

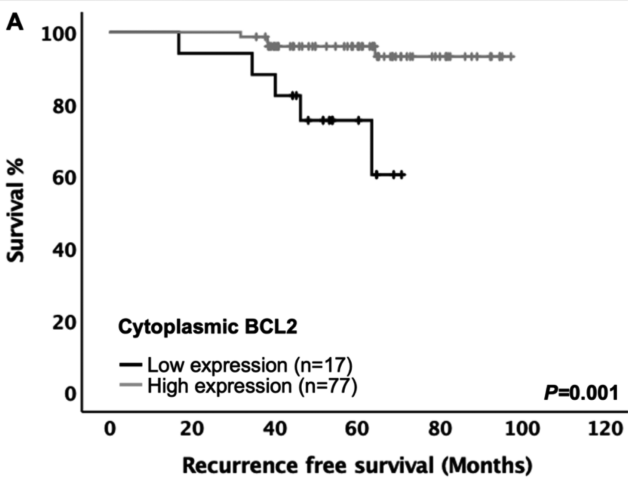

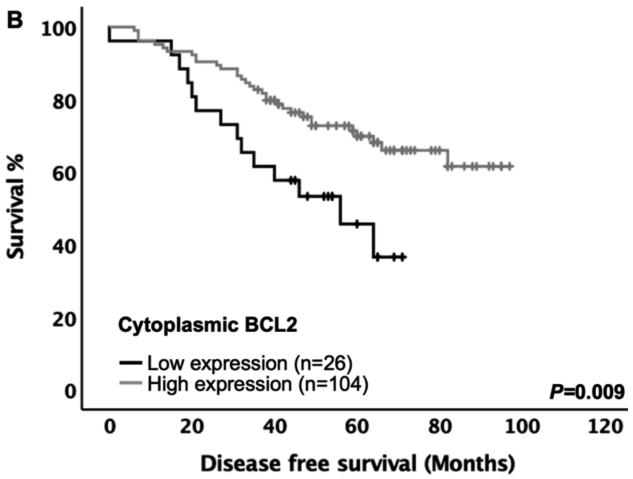

Fig. 9. Expression of BCL2 and clinical outcome in triple negative breast cancer. Kaplan-Meier curves showing associations of cytoplasmic BCL2 with recurrence free survival **(A)**, disease-free survival **(B)**.

encodes a 110 kD transmembrane glycoprotein that is highly expressed by human monocytes and tissue macrophages. CD68 is recognized as a pan-macrophage marker in various cancer types including BC (Mahmoud et al., 2012; Zhao et al., 2017). Several studies suggested that tumour cells stimulate macrophages to produce various factors that in turn stimulate tumour growth and survival (Bingle et al., 2002; Huang et al., 2002). IHC has revealed that TNBC has significantly more tumour-infiltrating macrophages compared to non-TNBCs (Lu et al., 2019). This study demonstrated high levels of CD68 cells in tumour nests and in TME were independent prognostic factor for OS.

These results are consistent with previous studies (Yuan et al., 2014; Wang et al., 2016), especially in the high infiltrated group (Wang et al., 2016). Patients with high CD68 infiltration express higher levels of IL-6 and CCL5 (Wang et al., 2016), which are well known to correlate with poor prognosis. However, little direct evidence reported the significance of the histological location of CD68 in BC except for a few studies (Mahmoud et al., 2012; Medrek et al., 2012; Ch'ng et al., 2013). In this study, CAIX protein expression was positively associated with high CD68 cells number in tumour nests. In invasive breast carcinoma, CD68+ accumulates at high density in hypoxic areas of tumours (Leek et al., 1999), and responds to hypoxia by secreting cytokines that promote cancer cell proliferation, angiogenesis, invasion and metastasis (Lewis and Murdoch, 2005). A significant correlation between CD68 and HIF-1α in patients with non-small cell lung cancer was reported (Jeong et al., 2019). The TAMs have different effects on tumour progression according to their histologic location. Leek et al. reported that hypoxia-associated tumour necrosis attracts macrophages into tumours, and these then contribute to angiogenesis and poor prognosis (Leek et al., 1999). The histological location of TAMs has been suggested to affect cancer progression, with stromal macrophages possibly impacting tubular architecture and tumour grade, and tumour nest macrophages aiding hypoxia-induced angiogenesis (Ch'ng et al., 2013). This could be explained by increased hypoxia and subsequent necrosis in the tumour centre as tumours outgrow their blood supply. This in turn could recruit and activate tumour nest macrophages which promotes angiogenesis and cancer progression. This stresses the roles of TAMs in both the tumour nest and the TME in cancer progression.

Another perhaps surprising finding in the present study was that HIF-1α gene in tumour compartment was up-regulated with high CAIX expression (log2 FC-0.274, P=0.012). HIF-1α gene codes HIF-1α, a transcriptional regulator in response to intra-tumoral hypoxia (Akanji et al., 2019; Hayashi et al., 2019), which plays an important role in cellular functions including apoptosis, cell proliferation, erythropoiesis, glucose metabolism, iron metabolism and angiogenesis. HIF-1α levels are significantly higher in invasive and poorly differentiated BCs as compared with well-differentiated cancers (Yamamoto et al., 2008; Stiehl et

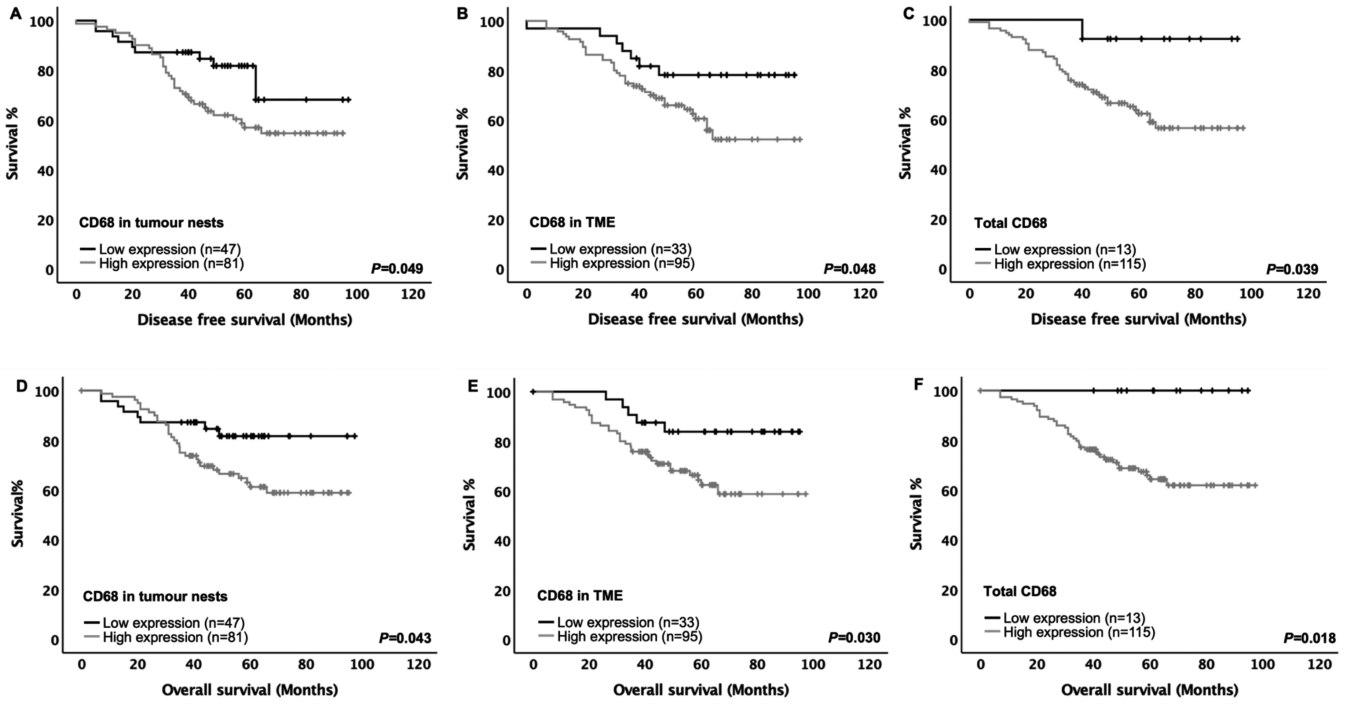

Fig. 10. Expression of CD68 and clinical outcome in triple negative breast cancer. Kaplan-Meier curves showing associations of CD68 in tumour nest, TME, and total CD68 with disease-free survival **(A-C)**, and overall survival **(D-F)**.

al., 2012). Specifically, increased levels of HIF-1α mRNA and the core hypoxic transcriptional response are associated with hormone receptor negative BC (Yamamoto et al., 2008). High expression of HIF-1α contributes to BC metastasis and malignant progression (Tosatto et al., 2016; Ponente et al., 2017; De Francesco et al., 2018; Ebright et al., 2020; Wyss et al., 2021) by acting at multiple levels of the metastatic cascade (Gilkes et al., 2014; Liu et al., 2015). It was suggested that targeting this pathway might provide a new therapeutic option for TNBC patients (Liu et al., 2015). Consistent with a recent meta-analysis, the present study has shown that overexpression of HIF-1α in BC predicts poor outcomes (Shamis et al., 2021). As determined by Chi-squared test, the expression of cytoplasmic HIF-1α was significantly associated with cytoplasmic CAIX. Results have been variable in other studies. CAIX expression has correlated with HIF-1α expression in some studies (Brennan et al., 2006), but not in others (Kuijper et al., 2005). When hypoxic environment advances, HIF-1α is overexpressed and promoting upregulation of various target genes, including CAIX allowing BC cells to undergo metabolic adaptation to hypoxia (Chen et al., 2010; Choi et al., 2013).

Within the tumour compartment, the resulting volcano plot (Fig. 6A) did not clearly differentiate between low and high CAIX expression groups. This might be due to the same tumour had TMA cores for stroma and for tumour sample that were stained together then scored separately and an average score was taken.

In addition, within PanCK- samples, CD3E showed high level by a log2 FC of 0.30, P=0.005 in low CAIX tumours compared to high CAIX tumours. Severe immune deficiency is associated with the CD3E subunit of CD3-encoded by the CD3E gene on chromosome 11 and is a routine target for CD3 antibodies (Benonisson et al., 2019; Iizuka et al., 2019). Studies have found that cancer patients with low CD3E mRNA levels tend to have poor prognosis (Punt et al., 2015; Lecerf et al., 2019). A recent study found that CD3E gene might be considered as novel and potential biomarkers of TNBC (Li et al., 2021). The location of CD3, whether in tumour nests or in TME is important. In the present study, higher infiltration of CD3 cells was observed in both tumour nests and TME of TNBC, which were uniformly significantly associated with favourable RFS. In line with previous results, the present study has shown that patients with high CD3+ infiltration predicted better survival than patients with low lymphocytic infiltration (Rathore et al., 2014; Wang et al., 2019). We found CD3 in TME to be a superior parameter. Based on this finding, we hypothesised that the TME plays the main role in antitumour activity. Studies of early-stage TNBC showed that TIL levels in the stromal compartment of TNBC tumours was higher than in lower-grade tumours and could improve the outcome, which is consistent with the present results (Salgado et al., 2015; Blackley and Loi, 2019). A purified anti-CD3E nanobody effectively inhibited the growth of BC *in vivo* (Moradi-Kalbolandi et al., 2020). Furthermore, a recombinant anti-CD3E nanobody effectively suppressed angiogenesis and tumour cell proliferation in a BC mouse model (Khatibi et al., 2019). In context of hypoxia, studies have reported that BC patients with poor outcomes had high HIF-1α

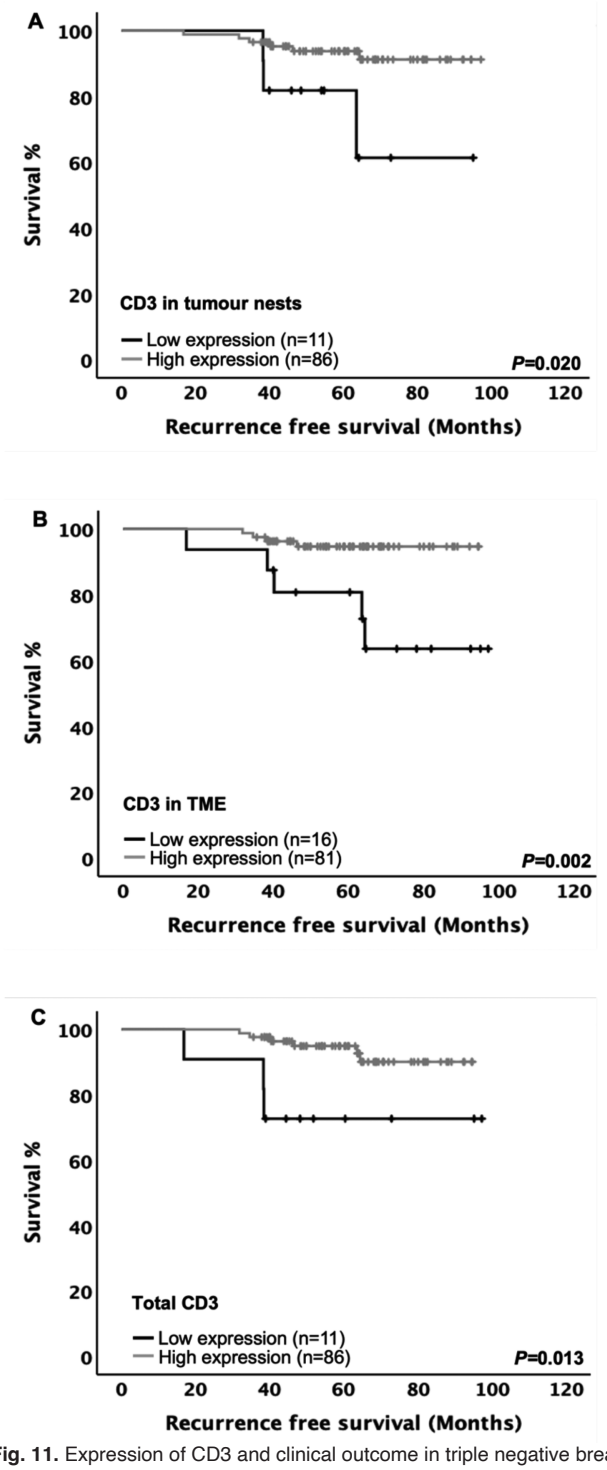

Fig. 11. Expression of CD3 and clinical outcome in triple negative breast cancer. Kaplan-Meier curves showing associations of CD3 in tumour nests **(A)**, in TME **(B)**, and total CD3 **(C)** with recurrence free survival.

and low expression of CD3E (Serganova et al., 2018), suggesting that hypoxia could reflect more aggressive disease and a more immunosuppressive tumour microenvironment. Indeed, higher CAIX expression was significantly associated with lower expression of CD3E in TNBC, and it was associated with worse OS (Chafe et al., 2019). Our observations were consistent with these results.

BCL2 was up-regulated in low CAIX tumours compared to high CAIX tumours (log2 FC 0.19, P=0.008). BCL2 protein, coded by the BCL2 gene (Tsujimoto et al., 1984), and plays an anti-apoptotic role and inhibits cell death (Vaux et al., 1988), causing in prolonged cell survival (McDonnell et al., 1989). BCL2 is overexpressed in many cancers and contributes to tumour initiation, progression, and therapy resistance (Tsujimoto et al., 1984; Ohmori et al., 1993; Kirkin et al., 2004). There is increasing evidence to suggest that BCL2 may be an effective therapy for many cancers (Klasa et al., 2002; Oltersdorf et al., 2005; Oakes et al., 2012). BCL2 is overexpressed in 80% of ER-positive BC whereas overexpressed in approximately 41% of TNBC cases (Merino et al., 2016). Yang et al. (2009) examined patients with early BC who underwent breast conservative surgery with radiotherapy and found that BCL2 expression associated with ipsilateral breast recurrence. Furthermore, BCL2 decreased expression was a good predictive factor for better chemotherapy response in BC patients (Yang et al., 2013). Bouchalova et al. (2015) postulated that overexpression of BCL2 was a significant independent predictor of poor prognosis in TNBC patients treated with anthracycline-based adjuvant chemotherapy. On the other hand, the reverse was observed in the present study, that high BCL2 expression by immune cells was significantly associated with improved survival rates in TNBC patients. Indeed, BCL2 expression has been reported as a favourable prognostic marker across multiple BC molecular subtypes (Hellemans et al., 1995; Sirvent et al., 2004; Callagy et al., 2008; Nadler et al., 2008; Hwang et al., 2012; Kim et al., 2012). BCL2 positive expression was associated with better survival of metastatic and early BC treated with either hormone therapy or chemotherapy (Gasparini et al., 1995; Tsutsui et al., 2006; Lee et al., 2007). With respect to TNBC, as extensively reviewed by Bouchalova et al. (2014), most clinical studies have shown that increased expression of BCL2 is connected with better survival for TNBC (Rhee et al., 2008; Dawson et al., 2010; Kallel-Bayoudh et al., 2011; Abdel-Fatah et al., 2013). The favourable clinical outcome in BCL2 positive cases is surprising considering the anti-apoptotic nature of BCL2. BCL2 functions not only in apoptosis, but also in the cell cycle where cell line studies have shown that its expression hinder G1 progression and G1-S transition. This is due to it extending the G0 phase. Furthermore, it has been shown to inhibit growth in a manner akin to p53 (Pietenpol et al.; 1994; O'Reilly et al., 1996; Zinkel et al., 2006). BCL2 expression in BC has also been found to be associated with markers of better prognosis. In fact, BCL2 is inversely correlated with proliferative markers, such as Ki67, and Her-2 overexpression, and with improved survival in BC (Joensuu et al., 1994). Therefore, BCL2 plays an antiproliferative role despite its antiapoptotic effect (Knowlton et al., 1998, Mitrović et al., 2014), resulting in a more favourable outcome compared to that of BC with BCL2-negative expression. Also, a variety of studies have suggested that it may undergo conversion from protector to killer under some circumstances. For example, proteolytic removal of N-terminal sequences by caspase-mediated cleavage reverses the phenotype of BCL2 (Cheng et al., 1997). Furthermore, this role may be explained by its interactions with other members of the BCL2 family of apoptotic regulators, especially with proapoptotic proteins (Redondo, 2013). HIF-1α can initiate hypoxia mediated apoptosis by increasing the expression of BCL2 binding proteins (BNIP3 and NIX), thereby inhibiting the anti-apoptotic effect of BCL2, or by stabilising wild-type p53 if the cell already has a p53 gene mutation. Also, the severity of hypoxia determines whether cells become apoptotic or adapt to hypoxia and survive (Greijer and Van der Wall, 2004).

In the present study, it was apparent that tumour hypoxia has an essential role in regulating tumour inflammatory cell functions in addition to regulating immune cell recruitment. The epithelial and stromal genes expression was readily delineated by CAIX expression in TNBC. Analysis of genes expression in tumour cells showed hypoxia increased expression of CD68 which contribute to tumour progression and are associated with poor tumour prognosis. Analysis of genes expression in the stroma showed that immune cells (CD3, BCL2) were down-regulated with hypoxia that have the potential for antitumor effects.

Acidification of the microenvironment enhances the tumour cell migration, invasion and the radio-resistance (Corbet and Feron, 2017), and reduces antitumour immunity in many ways. Increased levels of H+ and lactate decrease the capacity of T cells to produce interleukin-2 (IL-2), interferon-γ (IFNγ), granzyme B and perforin and that of monocytes to release tumour necrosis factor (TNF) in a dose-dependent manner. The acidic microenvironment also decreases the activity of NK cells. Thus, hypoxia-driven tumour acidification is a formidable barrier to immune cell function (Samuvel et al., 2009; Dietl et al., 2010; Wang et al., 2014). The data from the present study highlight hypoxia and inflammation as critical modulators of the immune microenvironment of solid tumours. Hypoxia increases the cellular plasticity and tumour heterogeneity and cancer cells immune suppression (Terry et al., 2018).

Well-controlled future studies are required to overcome the limitations of the present study. These include studies with a larger sample size of TNBC tissues. Also, some of the patients are represented by multiple cores across the TMAs sections, further validation using full tissue sections would enable insight

into any spatial heterogeneity of CAIX-signature across each patient. Furthermore, whole transcriptome profiling is warranted. Finally, the high expression of CD68 in the cytokeratin-positive AOIs in the transcriptomic analysis highlights a key limitation of the approach. Presumably this reflects the lack of single cell resolution to distinguish between tumour and immune cells within tumour nests as high CAIX expression is positively correlated with CD68 staining in tumour nests and not the TME. Therefore, newer technology such as CosMx could be used to investigate gene and protein expression at the single cell level.

Conclusion

A specific mRNA signature associated with hypoxia within tumour and stromal compartments was identified in TNBC using spatial transcriptomic technology. This may influence tumour development, and thus represent potential targets for novel intervention strategies. Three DEGs were identified in tumour compartment and nine DEGs in the stromal compartment in comparison of high and low CAIX expression groups. Four genes were selected to validated by IHC at protein level in microarray TNBC datasets. IHC staining showed tumour infiltrating macrophage can predict the progression of TNBC and the involvement of BCL2 and lymphocyte in tumour protection. IHC proteins expression were associated with a different prognosis in TNBC. High HIF-1α, and CD68 expression in tumour were linked to poorer survival while high levels of CD3 and BCL2 expression within stroma were associated with improved patient's survival. In addition, high density CD68 in both tumour nests and TME were independently predictive of OS. Among the four markers tested, HIF-1α and CD68 expression had a significant positive association with CAIX expression whereas BCL2 expression showed significant inverse association with CAIX expression. These results demonstrate that even from a small number of samples, spatial transcriptomic profiling using the GeoMx DSP can be used as an efficient tool to identify potential prognostic biomarkers that may have clinical relevance, however, further functional analysis of these results is warranted.

Acknowledgements. Acknowledge the support of NHS Research Scotland (NRS) (NHS GGC Biorepository) for providing access to the clinical specimens and Glasgow Tissue Research Facility for TMA construction. The contribution of Julie Doughty is also acknowledge.

Author contributions statement. J.E and D.M conceived and planned the study. E.M is a consultant pathologist advising on all pathology and TMA construction. F.S collected clinical samples and the data. S.S carried out the experiment, scored TMAs, analysed the data and wrote the manuscript. S.A aided in double scoring TMAs. A.A stained immune markers. N.J designed the GeoMx experiments. H.L and P.H performed the GeoMx analysis. J.E and D.M supervised the findings of this work and aided in editing the manuscript. All the authors have read and approved the manuscript.

Ethics approval. This study was approved by the Research Ethics Committee of the West Glasgow University Hospitals NHS Trust (NHS GG&C REC reference: 16/WS/0207), in accordance with Human Tissue (Scotland) Act 2006.The material used was taken from the Pathology Diagnostic archive and as such, unconsented surplus rather than project specific material and that these samples were used without consent following the HTA legislation on consent exemption.

Availability of data and materials. The data and materials analysed during this study have been deposited in Enlighten and are accessible at: http://researchdata.gla.ac.uk/id/eprint/1333

Competing interests. The authors declare no conflicts of interest.

Funding information. This research was funded by Libyan government and Libyan Cultural Affairs Bureau (Grant no. AA274-518-54090). Funding CRUK Clinician Scientist Award (C55370/A25813; N.J).

References

Abdel-Fatah T.M.A., Perry C., Dickinson P., Ball G., Moseley P., Madhusudan S., Ellis I.O. and Chan S. (2013). Bcl2 is an independent prognostic marker of triple negative breast cancer (TNBC) and predicts response to anthracycline combination (ATC) chemotherapy (CT) in adjuvant and neoadjuvant settings. Ann. Oncol. 24, 2801-2807.

Ahn K.J., Park J. and Choi Y. (2017). Lymphovascular invasion as a negative prognostic factor for triple-negative breast cancer after surgery. Radiat. Oncol. J. 35, 332-339.

Akanji M.A., Rotimi D. and Adeyemi O.S. (2019). Hypoxia-inducible factors as an alternative source of treatment strategy for cancer. Oxid. Med. Cell. Longev. 2019, 8547846.

Bankhead P., Loughrey M.B., Fernández J.A., Dombrowski Y., McArt D.G., Dunne P.D., McQuaid S., Gray R.T., Murray L.J. and Coleman H.G. (2017). QuPath: Open source software for digital pathology image analysis. Sci. Rep. 7, 16878.

Bareche Y., Buisseret L., Gruosso T., Girard E., Venet D., Dupont F., Desmedt C., Larsimont D., Park M., Rothé F., Stagg J. and Sotiriou C. (2020). Unraveling triple-negative breast cancer tumor microenvironment heterogeneity: Towards an optimized treatment approach. J. Natl. Cancer Inst. 112, 708-719.

Beasley N.J., Wykoff C.C., Watson P.H., Leek R., Turley H., Gatter K., Pastorek J., Cox G.J., Ratcliffe P. and Harris A.L. (2001). Carbonic anhydrase IX, an endogenous hypoxia marker, expression in head and neck squamous cell carcinoma and its relationship to hypoxia, necrosis, and microvessel density. Cancer Res. 61, 5262-5267.

Benonisson H., Altıntaş I., Sluijter M., Verploegen S., Labrijn A.F., Schuurhuis D.H., Houtkamp M.A., Verbeek J.S., Schuurman J. and van Hall T. (2019). CD3-bispecific antibody therapy turns solid tumors into inflammatory sites but does not install protective memory. Mol. Cancer Ther. 18, 312-322.

Bianchini G., Balko J.M., Mayer I.A., Sanders M.E. and Gianni L. (2016). Triple-negative breast cancer: challenges and opportunities of a heterogeneous disease. Nat. Rev. Clin. Oncol. 13, 674-690.

Bingle L., Brown N.J. and Lewis C.E. (2002). The role of tumour-associated macrophages in tumour progression: implications for new anticancer therapies. J. Pathol. 196, 254-265.

Blackley E.F. and Loi S. (2019). Targeting immune pathways in breast cancer: review of the prognostic utility of TILs in early stage triple negative breast cancer (TNBC). Breast 48, (Suppl 1) S44-S48.

Bouchalova K., Kharaishvili G., Bouchal J., Vrbkova J., Megova M. and Hlobilkova A. (2014). Triple negative breast cancer-BCL2 in prognosis and prediction. Review. Curr. Drug Targets 15, 1166-1175.

Bouchalova K., Svoboda M., Kharaishvili G., Vrbkova J., Bouchal J., Trojanec R., Koudelakova V., Radova L., Cwiertka K. and Hajduch M. (2015). BCL2 is an independent predictor of outcome in basal-like triple-negative breast cancers treated with adjuvant anthracycline-based chemotherapy. Tumor Biol. 36, 4243-4252.

Bray F., Ferlay J., Soerjomataram I., Siegel R.L., Torre L.A. and Jemal A. (2018). Global cancer statistics 2018: GLOBOCAN estimates of incidence and mortality worldwide for 36 cancers in 185 countries. CA Cancer J. Clin. 68, 394-424.

Brennan D.J., Jirstrom K., Kronblad A., Millikan R.C., Landberg G., Duffy M.J., Rydén L., Gallagher W.M. and O'Brien S.L. (2006). CA IX is an independent prognostic marker in premenopausal breast cancer patients with one to three positive lymph nodes and a putative marker of radiation resistance. Clin. Cancer Res. 12, 6421-6431.

Callagy G.M., Webber M.J., Pharoah P.D.P. and Caldas C. (2008). Meta-analysis confirms BCL2 is an independent prognostic marker in breast cancer. BMC Cancer 8, 153.

Ch'ng, E. S., Tuan Sharif S.E.T. and Jaafar H. (2013). In human invasive breast ductal carcinoma, tumor stromal macrophages and tumor nest macrophages have distinct relationships with clinicopathological parameters and tumor angiogenesis. Virchows Arch. 462, 257-267.

Chafe S.C., McDonald P.C., Saberi S., Nemirovsky O., Venkateswaran G., Burugu S., Gao D., Delaidelli A., Kyle A.H., Baker J.H.E., Gillespie J.A., Bashashati A., Minchinton A.I., Zhou Y., Shah S. and Dedhar S. (2019). Targeting hypoxia-induced carbonic anhydrase IX enhances immune-checkpoint blockade locally and systemically. Cancer Immunol. Res. 7, 1064-1078.

Chen C.-L., Chu J.-S., Su W.-C., Huang S.-C. and Lee W.-Y. (2010). Hypoxia and metabolic phenotypes during breast carcinogenesis: expression of HIF-1α, GLUT1, and CAIX. Virchows Archiv. 457, 53-61.

Cheng E.H., Kirsch D.G., Clem R.J., Ravi R., Kastan M.B., Bedi A., Ueno K. and Hardwick J.M. (1997). Conversion of Bcl-2 to a Bax-like death effector by caspases. Science 278, 1966-1968.

Choi J., Jung W.-H. and Koo J.S. (2013). Metabolism-related proteins are differentially expressed according to the molecular subtype of invasive breast cancer defined by surrogate immunohistochemistry. Pathobiology 80, 41-52.

Corbet C. and Feron O. (2017). Tumour acidosis: from the passenger to the driver's seat. Nat. Rev. Cancer 17, 577-593.

Cui J. and Jiang H. (2019). Prediction of postoperative survival of triple-negative breast cancer based on nomogram model combined with expression of HIF-1α and c-myc. Medicine (Baltimore) 98, e17370.

Dawson S.-J., Makretsov N., Blows F.M., Driver K.E., Provenzano E., Le Quesne J., Baglietto L., Severi G., Giles G.G., McLean C.A., Callagy G., Green A.R., Ellis I., Gelmon K., Turashvili G., Leung S., Aparicio S., Huntsman D. Caldas C. and Pharoah P. (2010). BCL2 in breast cancer: a favourable prognostic marker across molecular subtypes and independent of adjuvant therapy received. Br. J. Cancer 103, 668-675.

De Francesco E.M., Maggiolini M. and Musti A.M. (2018). Crosstalk between Notch, HIF-1α and GPER in breast cancer EMT. Int. J. Mol. Sci. 19, 2011.

Denkert C., von Minckwitz G., Darb-Esfahani S., Lederer B., Heppner B.I., Weber K.E., Budczies J., Huober J., Klauschen F. and Furlanetto J. (2018). Tumour-infiltrating lymphocytes and prognosis in different subtypes of breast cancer: a pooled analysis of 3771 patients treated with neoadjuvant therapy. Lancet Oncol. 19, 40-50.

Dietl K., Renner K., Dettmer K., Timischl B., Eberhart K., Dorn C., Hellerbrand C., Kastenberger M., Kunz-Schughart L.A., Oefner P.J., Andreesen R., Gottfried E. and Kreutz M.P. (2010). Lactic acid and acidification inhibit TNF secretion and glycolysis of human monocytes. J. Immunol. 184, 1200-1209.

Ebright R.Y., Zachariah M.A., Micalizzi D.S., Wittner B.S., Niederhoffer K.L., Nieman L.T., Chirn B., Wiley D.F., Wesley B., Shaw B., Nieblas-Bedolla E., Atlas L., Szabolcs A., Iafrate J.A., Toner M., Ting D.T., Brastianos P.K., Haber D.A. and Maheswaran S. (2020). HIF1A signaling selectively supports proliferation of breast cancer in the brain. Nat. Commun. 11, 1-13.

Gasparini G., Barbareschi M., Doglioni C., Palma P.D., Mauri F.A., Boracchi P., Bevilacqua P., Caffo O., Morelli L., Verderio P., Pezzella F. and Harris L. (1995). Expression of bcl-2 protein predicts efficacy of adjuvant treatments in operable node-positive breast cancer. Clin. Cancer Res. 1, 189-198.

Gilkes D.M., Semenza G.L. and Wirtz D. (2014). Hypoxia and the extracellular matrix: drivers of tumour metastasis. Nat. Rev. Cancer. 14, 430-439.

Goldhirsch A., Winer E.P., Coates A.S., Gelber R.D., Piccart-Gebhart M., Thürlimann B., Senn H.-J., Albain K.S., André F., Bergh J., Bonnefoi H., Bretel-Morales D., Burstein H., Cardoso F., Castiglione-Gertsch M., Coates A.S., Colleoni M., Costa A., Curigliano G., Davidson N.E., Di Leo A., Ejlertsen B., Forbes J.F., Gelber R.D., Gnant M., Goldhirsch A., Goodwin P., Goss P.E., Harris J.R., Hayes D.F., Hudis C.A., Ingle J.N., Jassem J., Jiang Z., Karlsson P., Loibl S., Morrow M., Namer M., Osborne C.K., Partridge A.H., Penault-Llorca F., Perou C.M., Piccart-Gebhart M.J., Pritchard K.I., Rutgers E.J.T., Sedlmayer F., Semiglazov V., Shao Z.-M., Smith I., Thürlimann B., Toi M., Tutt A., Untch M., Viale G., Watanabe T., Wilcken N., Winer E.P. and Wood W.C. (2013). Personalizing the treatment of women with early breast cancer: highlights of the St Gallen International Expert Consensus on the Primary Therapy of Early Breast Cancer 2013. Ann. Oncol. 24, 2206-2223.

Greijer A.E. and Van der Wall E. (2004). The role of hypoxia inducible factor 1 (HIF-1) in hypoxia induced apoptosis. J. Clin. Pathol. 57, 1009-1014.

Hanahan D. and Weinberg R.A. (2011). Hallmarks of cancer: the next generation. Cell 144, 646-674.

Hayashi Y., Yokota A., Harada H. and Huang G. (2019). Hypoxia/pseudohypoxia-mediated activation of hypoxia-inducible factor-1α in cancer. Cancer Sci. 110, 1510-1517.

Hellemans P., Van Dam P.A., Weyler J., Van Oosterom A., Buytaert P. and Van Marck E. (1995). Prognostic value of bcl-2 expression in invasive breast cancer. Br. J. Cancer 72, 354-360.

Huang S., Van Arsdall M., Tedjarati S., McCarty M., Wu W., Langley R. and Fidler I.J. (2002). Contributions of stromal metalloproteinase-9 to angiogenesis and growth of human ovarian carcinoma in mice. J. Natl. Cancer Inst. 94, 1134-1142.

Hwang K.-T., Woo J.W., Shin H.C., Kim H.S., Ahn S.K., Moon H.-G., Han W., Park I.A. and Noh D.-Y. (2012). Prognostic influence of BCL2 expression in breast cancer. Int. J. Cancer 131, E1109-E1119.

Iizuka A., Nonomura C., Ashizawa T., Kondou R., Ohshima K., Sugino T., Mitsuya K., Hayashi N., Nakasu Y., Maruyama K., Yamaguchi K. and Akiyama Y. (2019). A T-cell-engaging B7-H4/CD3-bispecific Fab-scFv antibody targets human breast cancer. Clin. Cancer Res.

25, 2925-2934.

Jeong H., Kim S., Hong B.-J., Lee C.-J., Kim Y.-E., Bok S., Oh J.-M., Gwak S.-H., Yoo M.Y., Lee M.S., Chung S.-J., Defrêne J., Tessier P., Pelletier M., Jeon H., Roh T.-Y., Kim B., Kim K.H., Ju J.H., Kim S., Lee Y.-J., Kim D.-W., Kim I.H., Kim H.J., Park J.-W., Lee Y.-S., Lee J.S., Cheon G.J., Weissman I.L., Chung D.H., Jeon Y.K. and Ahn G.-O. (2019). Tumor-associated macrophages enhance tumor hypoxia and aerobic glycolysis. Cancer Res. 79, 795-806.

Jin M.-S., Lee H., Park I.A., Chung Y.R., Im S.-A., Lee K.-H., Moon H.-G., Han W., Kim K., Kim T.-Y. and Noh D.-Y. (2016). Overexpression of HIF1α and CAXI predicts poor outcome in early-stage triple negative breast cancer. Virchows Archiv. 469, 183-190.

Joensuu H., Pylkkänen L. and Toikkanen S. (1994). Bcl-2 protein expression and long-term survival in breast cancer. Am. J. Pathol. 145, 1191-1198.

Kallel-Bayoudh I., Hassen H.B., Khabir A., Boujelbene N., Daoud J., Frikha M., Sallemi-Boudawara T., Aifa S. and Rebaï A. (2011). Bcl-2 expression and triple negative profile in breast carcinoma. Med. Oncol. 28, 55-61.

Khatibi A.S., Roodbari N.H., Majidzade-A K., Yaghmaei P. and Farahmand L. (2019). *In vivo* tumor-suppressing and anti-angiogenic activities of a recombinant anti-CD3ε nanobody in breast cancer mice model. Immunotherapy 11, 1555-1567.

Kim H.S., Moon H.-G., Han W., Yom C.K., Kim W.H., Kim J.H. and Noh D.-Y. (2012). COX2 overexpression is a prognostic marker for Stage III breast cancer. Breast Cancer Res. Treat. 132, 51-59.

Kim H., Lin Q., Glazer P.M. and Yun Z. (2018). The hypoxic tumor microenvironment in vivo selects the cancer stem cell fate of breast cancer cells. Breast Cancer Res. 20, 1-15.

Kirkegaard T., Edwards J., Tovey S., McGlynn L.M., Krishna S.N., Mukherjee R., Tam L., Munro A.F., Dunne B. and Bartlett J.M.S. (2006). Observer variation in immunohistochemical analysis of protein expression, time for a change? Histopathology 48, 787-794.

Kirkin V., Joos S. and Zörnig M. (2004). The role of Bcl-2 family members in tumorigenesis. Biochim. Biophys. Acta 1644, 229-249.

Klasa R.J., Gillum A.M., Klem R.E. and Frankel S.R. (2002). Oblimersen Bcl-2 antisense: facilitating apoptosis in anticancer treatment. Antisense Nucleic Acid Drug Dev. 12, 193-213.

Klintrup K., Mäkinen J.M., Kauppila S., Väre P.O., Melkko J., Tuominen H., Tuppurainen K., Mäkelä J., Karttunen T.J. and Mäkinen M.J. (2005). Inflammation and prognosis in colorectal cancer. Eur. J. Cancer 41, 2645-2654.

Knowlton K., Mancini M., Creason S., Morales C., Hockenbery D. and Anderson B.O. (1998). Bcl-2 slows *in vitro* breast cancer growth despite its antiapoptotic effect. J. Surg. Res. 76, 22-26.

Koo T.K. and Li M.Y. (2016). A guideline of selecting and reporting intraclass correlation coefficients for reliability research. J. Chirop. Med. 15, 155-163.

Kuijper A., van der Groep P., van der Wall E. and van Diest P.J. (2005). Expression of hypoxia-inducible factor 1 alpha and its downstream targets in fibroepithelial tumors of the breast. Breast Cancer Res. 7, 1-11.

Lal A., Peters H., St. Croix B., Haroon Z.A., Dewhirst M.W., Strausberg R.L., Kaanders J.H., Van Der Kogel A.J. and Riggins G.J. (2001). Transcriptional response to hypoxia in human tumors. J. Natl. Cancer Inst. 93, 1337-1343.

Lecerf C., Kamal M., Vacher S., Chemlali W., Schnitzler A., Morel C., Dubot C., Jeannot E., Meseure D., Klijanienko J., Mariani O., Borcoman E., Calugaru V., Badois N., Chilles A., Lesnik M., Krhili S., Choussy O., Hoffmann C., Piaggio E., Bieche I. and Le Tourneau C. (2019). Immune gene expression in head and neck squamous cell carcinoma patients. Eur. J. Cancer 121, 210-223.

Lee K.-H., Im S.-A., Oh D.-Y., Lee S.-H., Chie E.K., Han W., Kim D.-W., Kim T.-Y., Park I.A., Noh D.-Y., Heo D.S., Ha S.W. and Bang Y.-J. (2007). Prognostic significance of bcl-2 expression in stage III breast cancer patients who had received doxorubicin and cyclophosphamide followed by paclitaxel as adjuvant chemotherapy. BMC Cancer 7, 1-9.

Leek R.D., Landers R.J., Harris A.L. and Lewis C.E. (1999). Necrosis correlates with high vascular density and focal macrophage infiltration in invasive carcinoma of the breast. Br. J. Cancer 79, 991-995.

Lei S., Zheng R., Zhang S., Wang S., Chen R., Sun K., Zeng H., Zhou J. and Wei W. (2021). Global patterns of breast cancer incidence and mortality: A population-based cancer registry data analysis from 2000 to 2020. Cancer Commun (Lond). 41, 1183-1194.

Lewis C. and Murdoch C. (2005). Macrophage responses to hypoxia: implications for tumor progression and anti-cancer therapies. Am. J. Pathol. 167, 627-635.

Li M.-X., Jin L.-T., Wang T.-J., Feng Y.-J., Pan C.-P., Zhao D.-M. and Shao J. (2018). Identification of potential core genes in triple negative breast cancer using bioinformatics analysis. Onco Targets Ther. 11, 4105-4105.

Li L., Huang H., Zhu M. and Wu J. (2021). Identification of hub genes and pathways of triple negative breast cancer by expression profiles analysis. Cancer Manag. Res. 13, 2095-2104.

Liu Z.-J., Semenza G.L. and Zhang H.F. (2015). Hypoxia-inducible factor 1 and breast cancer metastasis. J. Zhejiang Univ. Sci. B. 16, 32-43.

Loi S., Michiels S., Salgado R., Sirtaine N., Jose V., Fumagalli D., Kellokumpu-Lehtinen P.-L., Bono P., Kataja V., Desmedt C., Piccart M.J., Loibl S., Denkert C., Smyth M.J., Joensuu H. and Sotiriou C. (2014). Tumor infiltrating lymphocytes are prognostic in triple negative breast cancer and predictive for trastuzumab benefit in early breast cancer: results from the FinHER trial. Ann. Oncol. 25, 1544-1550.

Lu X., Yang R., Zhang L., Xi Y., Zhao J., Wang F., Zhang H. and Li Z. (2019). Macrophage colony-stimulating factor mediates the recruitment of macrophages in triple negative breast cancer. Int. J. Biol. Sci. 15, 2859-2871.

Mahmoud S., Lee A., Paish E., Macmillan R., Ellis I. and Green A.R. (2012). Tumour-infiltrating macrophages and clinical outcome in breast cancer. J. Clin. Pathol. 65, 159-163.

Matsumoto H., Koo S.-I., Dent R., Tan P.H. and Iqbal J. (2015). Role of inflammatory infiltrates in triple negative breast cancer. J. Clin. Pathol. 68, 506-510.

McDonnell T.J., Deane N., Platt F.M., Nunez G., Jaeger U., McKearn J.P. and Korsmeyer S.J. (1989). bcl-2-immunoglobulin transgenic mice demonstrate extended B cell survival and follicular lymphoproliferation. Cell 57, 79-88.

Medrek C., Pontén F., Jirström K. and Leandersson K. (2012). The presence of tumor associated macrophages in tumor stroma as a prognostic marker for breast cancer patients. BMC Cancer 12, 306.

Merino D., Lok S., Visvader J. and Lindeman G. (2016). Targeting BCL-2 to enhance vulnerability to therapy in estrogen receptor-positive breast cancer. Oncogene 35, 1877-1887.

Mitrović O., Čokić V., Đikić D., Budeč M., Vignjević S., Subotički T., Gulan M., Radović S. and Furtula S. (2014). Correlation between

ER, PR, HER-2, Bcl-2, p53, proliferative and apoptotic indexes with HER-2 gene amplification and TOP2A gene amplification and deletion in four molecular subtypes of breast cancer. Target. Oncol. 9, 367-379.

Moradi-Kalbolandi S., Sharifi-K A., Darvishi B., Majidzadeh-A K., Jalili N., Sadeghi S., Mosayebzadeh M., Sanati H., Salehi M. and Farahmand L. (2020). Evaluation the potential of recombinant anti-CD3 nanobody on immunomodulatory function. Mol. Immunol. 118, 174-181.

Nadler Y., Camp R.L., Giltnane J.M., Moeder C., Rimm D.L., Kluger H.M. and Kluger Y. (2008). Expression patterns and prognostic value of Bag-1 and Bcl-2 in breast cancer. Breast Cancer Res. 10, R35.

Ni C., Yang L. Xu Q., Yuan H., Wang W., Xia W., Gong D., Zhang W. and Yu K. (2019). CD68-and CD163-positive tumor infiltrating macrophages in non-metastatic breast cancer: a retrospective study and meta-analysis. J. Cancer 10, 4463-4472.

Nwagu G.C., Bhattarai S., Swahn M., Ahmed S. and Aneja R. (2021). Prevalence and mortality of triple-negative breast cancer in west africa: Biologic and sociocultural factors. JCO Glob. Oncol. 7, 1129-1140.

O'Reilly L.A., Huang D.C. and Strasser A. (1996). The cell death inhibitor Bcl-2 and its homologues influence control of cell cycle entry. EMBO J. 15, 6979-6990.

Oakes S.R., Vaillant F., Lim E., Lee L., Breslin K., Feleppa F., Deb S., Ritchie M.E., Takano E., Ward T., Fox S.B., Generali D., Smyth G.K., Strasser A., Huang D.C.S., Visvader J.E. and Lindeman G.J. (2012). Sensitization of BCL-2–expressing breast tumors to chemotherapy by the BH3 mimetic ABT-737. Proc. Natl. Acad. Sci. USA 109, 2766-2771.

Ohmori T., Podack E.R., Nishio K., Takahashi M., Miyahara Y., Takeda Y., Kubota N., Funayama Y., Ogasawara H., Ohira T., Ohta S. and Saijo N. (1993). Apoptosis of lung cancer cells caused by some anti-cancer agents (MMC, CPT-11, ADM) is inhibited by BCL-2. Biochem. Biophys. Res. Commun. 192, 30-36.

Oltersdorf T., Elmore S.W., Shoemaker A.R., Armstrong R.C., Augeri D.J., Belli B.A., Bruncko M., Deckwerth T.L., Dinges J., Hajduk P.J., Joseph M.K., Kitada S., Korsmeyer S.J., Kunzer A.R., Letai A., Li C., Mitten M.J., Nettesheim D.G., Ng S., Nimmer P.M., O'Connor J.M., Oleksijew A., Petros A.M., Reed J.C., Shen W., Tahir S.K., Thompson C.B., Tomaselli K.J., Wang B., Wendt M.D., Zhang H., Fesik S.W. and Rosenberg S.H. (2005). An inhibitor of Bcl-2 family proteins induces regression of solid tumours. Nature 435, 677-681.

Pietenpol J.A., Papadopoulos N., Markowitz S., Willson J.K., Kinzler K.W. and Vogelstein B. (1994). Paradoxical inhibition of solid tumor cell growth by bcl2. Cancer Res. 54, 3714-3717.

Ponente, M., Campanini L., Cuttano R., Piunti A., Delledonne G.A., Coltella N., Valsecchi R., Villa A., Cavallaro U., Pattini L., Doglioni C. and Bernardi R. (2017). PML promotes metastasis of triple-negative breast cancer through transcriptional regulation of HIF1A target genes. JCI Insight 2, e87380.

Punt S., Houwing-Duistermaat J.J., Schulkens I.A., Thijssen V.L., Osse E.M., de Kroon C.D., Griffioen A.W., Fleuren G.J., Gorter A. and Jordanova E.S. (2015). Correlations between immune response and vascularization qRT-PCR gene expression clusters in squamous cervical cancer. Mol. Cancer 14, 71.

Rathore A.S., Kumar S., Konwar R., Makker A., Negi M.P.S. and Goel M.M. (2014). CD3+, CD4+ & CD8+ tumour infiltrating lymphocytes (TILs) are predictors of favourable survival outcome in infiltrating ductal carcinoma of breast. Indian J. Med. Res. 140, 361-369.

Redondo M. (2013). Bcl-2, an antiapoptotic gene indicator of good prognosis in breast cancer: The paradox. J. Carcinogene Mutagene 4, 134.

Rhee J., Han S.-W., Oh D.-Y., Kim J.H., Im S.-A., Han W., Park I.A., Noh D.-Y., Bang Y.-J. and Kim T.-Y. (2008). The clinicopathologic characteristics and prognostic significance of triple-negativity in node-negative breast cancer. BMC Cancer 8, 307.

Salgado R., Denkert C., Demaria S., Sirtaine N., Klauschen F., Pruneri G., Wienert S., Van den Eynden G., Baehner F.L., Pénault-Llorca F., Perez E.A., Thompson E.A., Symmans W.F., Richardson A.L., Brock J., Criscitiello C., Bailey H., Ignatiadis M., Floris G., Sparano J., Kos Z., Nielsen T., Rimm D.L., Allison K.H., Reis-Filho J.S., Loibl S., Sotiriou C., Viale G., Badve S., Adams S., Willard-Gallo K., Loi S. and International TILs Working Group 2014 (2015). The evaluation of tumor-infiltrating lymphocytes (TILs) in breast cancer: recommendations by an International TILs Working Group 2014. Ann. Oncol. 26, 259-271.

Samuvel D.J., Sundararaj K.P., Nareika A., Lopes-Virella M.F. and Huang Y. (2009). Lactate boosts TLR4 signaling and NF-κB pathway-mediated gene transcription in macrophages via monocarboxylate transporters and MD-2 up-regulation. J. Immunol. 182, 2476-2484.

Semenza G.L. (2003). Targeting HIF-1 for cancer therapy. Nat. Rev. Cancer 3, 721-732.

Serganova I., Cohen I.J., Vemuri K., Shindo M., Maeda M., Mane M., Moroz E., Khanin R., Satagopan J., Koutcher J.A. and Blasberg R. (2018). LDH-A regulates the tumor microenvironment via HIF-signaling and modulates the immune response. PLoS One 13, e0203965.

Shamis S.A., McMillan D.C. and Edwards J. (2021). The relationship between hypoxia-inducible factor 1α (HIF-1α) and patient survival in breast cancer: systematic review and meta-analysis. Crit. Rev. Oncol. Hematol. 159, 103231.

Shao C., Yang F., Miao S., Liu W., Wang C., Shu Y. and Shen H. (2018). Role of hypoxia-induced exosomes in tumor biology. Mol. Cancer 17, 120.

Sirvent J., Aguilar M.C., Olona M., Pelegrí A., Blázquez S. and Gutierrez C. (2004). Prognostic value of apoptosis in breast cancer (pT1-pT2). A TUNEL, p53, bcl-2, bag-1 and Bax immunohistochemical study. Histol. Histopathol. 19, 759-770.

Stewart R.L., Matynia A.P., Factor R.E. and Varley K.E. (2020). Spatially-resolved quantification of proteins in triple negative breast cancers reveals differences in the immune microenvironment associated with prognosis. Sci. Rep. 10, 6598.

Stiehl D.P., Bordoli M.R., Abreu-Rodríguez I., Wollenick K., Schraml P., Gradin K., Poellinger L., Kristiansen G. and Wenger R.H. (2012). Non-canonical HIF-2α function drives autonomous breast cancer cell growth via an AREG–EGFR/ErbB4 autocrine loop. Oncogene 31, 2283-2297.

Terry S., Zaarour R.F., Venkatesh G.H., Francis A., El-Sayed W., Buart S., Bravo P., Thiery J. and Chouaib S. (2018). Role of hypoxic stress in regulating tumor immunogenicity, resistance and plasticity. Int. J. Mol. Sci. 19, 3044.

Thiry A., Dogne J.-M., Masereel B. and Supuran C.T. (2006). Targeting tumor-associated carbonic anhydrase IX in cancer therapy. Trends Pharmacol. Sci. 27, 566-573.

Tosatto A., Sommaggio R., Kummerow C., Bentham R.B., Blacker T.S., Berecz T., Duchen M.R., Rosato A., Bogeski I., Szabadkai G.,

Rizzuto R. and Mammucari C. (2016). The mitochondrial calcium uniporter regulates breast cancer progression via HIF-1α. EMBO Mol. Med. 8, 569-585.

Tsujimoto Y., Finger L.R., Yunis J., Nowell P.C. and Croce C.M. (1984). Cloning of the chromosome breakpoint of neoplastic B cells with the t (14; 18) chromosome translocation. Science 226, 1097-1099.

Tsutsui S., Yasuda K., Suzuki K., Takeuchi H., Nishizaki T., Higashi H. and Era S. (2006). Bcl-2 protein expression is associated with p27 and p53 protein expressions and MIB-1 counts in breast cancer. BMC Cancer 6, 187.

Vaux D.L., Cory S. and Adams J.M. (1988). Bcl-2 gene promotes haemopoietic cell survival and cooperates with c-myc to immortalize pre-B cells. Nature 335, 440-442.

Wang T., Liu G. and R. Wang R. (2014). The intercellular metabolic interplay between tumor and immune cells. Front. Immunol. 5, 358.

Wang J., Chen H., Chen X. and Lin H. (2016). Expression of tumor-related macrophages and cytokines after surgery of triple-negative breast cancer patients and its implications. Med. Sci. Monit. 22, 115-120.

Wang Q., Li P. and Wu W. (2019). A systematic analysis of immune genes and overall survival in cancer patients. BMC Cancer 19, 1225.

Wu L., Yi B., Wei S., Rao D., He Y., Naik G., Bae S., Liu X.M., Yang W.-H., Sonpavde G., Liu R. and Wang L. (2019). Loss of FOXP3 and TSC1 accelerates prostate cancer progression through synergistic transcriptional and posttranslational regulation of c-MYC. Cancer Res. 79, 1413-1425.

Wyss C.B., Duffey N., Peyvandi S., Barras D., Usatorre A.M., Coquoz O., Romero P., Delorenzi M., Lorusso G. and Rüegg C. (2021). Gain of HIF1 activity and loss of miRNA let-7d promote breast cancer metastasis to the brain via the PDGF/PDGFR axis. Cancer Res. 81, 594-605.

Yamamoto Y., Ibusuki M., Okumura Y., Kawasoe T., Kai K., Iyama K. and Iwase H. (2008). Hypoxia-inducible factor 1α is closely linked to an aggressive phenotype in breast cancer. Breast Cancer Res. Treat. 110, 465-475.

Yang Q., Moran M.S. and Haffty B.G. (2009). Bcl-2 expression predicts local relapse for early-stage breast cancer receiving conserving surgery and radiotherapy. Breast Cancer Res. Treat. 115, 343-348.

Yang D., Chen M.-B., Wang L.-Q., Yang L., Liu C.-Y. and Lu P.-H. (2013). Bcl-2 expression predicts sensitivity to chemotherapy in breast cancer: a systematic review and meta-analysis. J. Exp. Clin. Cancer Res. 32, 1-11.

Yu T. and Di G. (2017). Role of tumor microenvironment in triple-negative breast cancer and its prognostic significance. Chin. J. Cancer Res. 29, 237-252.

Yuan Z.-Y., Luo R.-Z., Peng R.-J., Wang S.-S. and Xue C. (2014). High infiltration of tumor-associated macrophages in triple-negative breast cancer is associated with a higher risk of distant metastasis. Onco Targets Ther. 7, 1475-1480.

Zhao X., Qu J., Sun Y., Wang J., Liu X., Wang F., Zhang H., Wang W., Ma X., Gao X. and Zhang S. (2017). Prognostic significance of tumor-associated macrophages in breast cancer: a meta-analysis of the literature. Oncotarget 8, 30576-30586.

Zinkel S., Gross A. and Yang E. (2006). BCL2 family in DNA damage and cell cycle control. Cell Death Differ. 13, 1351-1359.

Accepted July 31, 2023